Review

Propellants, Explosives, Pyrotechnics

DOI: 10.1002/prep.201800253

Insensitive High Explosives: III. Nitroguanidine – Synthesis – Structure – Spectroscopy – Sensitiveness

Ernst-Christian Koch*[a]

Abstract: This paper reviews the production, synthesis, crystallography, particle morphology and spectroscopy of the insensitive high explosive nitroguanidine, (NGu, $CH_4N_4O_2$), CAS-No: [556-88-7] and its isotopologues [$^2D_4$]-NGu and [$^{15}N_4$]-NGu]. When compared with standard insensitive high explosives such as 1,3,5-triamino-2,4,6-trinitrobenzene (TATB), 1,1-diamino-2,2-dinitroethylene (FOX-7) and *N*-guanylurea dinitramide (FOX-12), Nitroguanidine proves to be the least sensitive. The review gives 170 references to the public domain. For Part II see ref. [1].

Keywords: Nitroguanidine · Nitrimine · Guanidinium nitrate · Insensitive Munitions · Sensitiveness

1 Introduction

Nitroguanidine is an important ingredient in triple base and insensitive, low erosion gun propellants, rocket propellants, gas generators for automobile restraint systems, smoke free pyrotechnics and shock insensitive high explosives [2]. Though nitroguanidine is a frequently used energetic material in said different roles it lacks a comprehensive review of its synthesis, structure, spectroscopy and sensitiveness.

Nitroguanidine (NGu) (**2**) has been prepared for the first time by *Jousselin* [3] through action of concentrated sulphuric acid on guanidinium nitrate (GuN) (**1**) in 1877 (Scheme 1). However, he did not correctly identify nitroguanidine but due to an erroneous nitrogen determination misinterpreted NGu for nitrosoguanidine, CAS-No: [674–81–7]. Hence both *Pellizzari* [4] and *Thiele* [5] are credited with the first correct identification of nitroguanidine in 1891 and 1892 respectively.

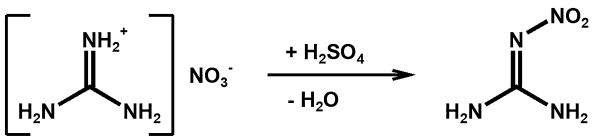

1 2

Scheme 1. *Jousselin's* Synthesis of Nitroguanidine later also applied by *Pellizzari* and *Thiele*.

Nitroguanidine is a nitrimine – see structure **A** in Figure 1 – but despite clear scientific evidence [6] also in terms of reactivity and spectroscopic data has long been falsely described as a nitramine – see structure **B** in Figure 1.

NGu possesses the same vicinal amino-nitro-arrangement as a number of other insensitive high explosives including FOX-7 (1,1-diamino-2,2-dinitroethylene) [7,8], TATB (1,3,5-triamino-2,4,6-trinitrobenzene) [9] or LLM-116 (4-amino-3,5-dinitro-1*H*-pyrazole) [10] as is depicted in Figure 2.

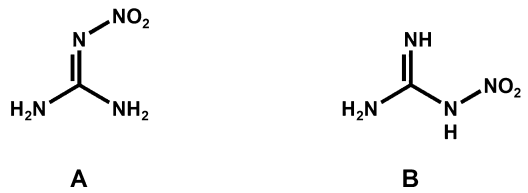

A B

Figure 1. Correct nitrimine structure **A** (left) and wrong nitramine structure **B** (right).

2 Nomenclature and Property Briefs

The IUPAC name for nitroguanidine is *2-nitroguanidine*. Other names include *„Petrolite"*, *„Guanite"* or *„Picrite"*. Sometimes nitroguanidine is misspelled in the English literature with a „**q**" in lieu of „**g**" (which both admittedly may look similar in hand writing) forming the word *„nitro**q**uanidine"* and possibly explaining the etymology of the acronym *„NQ"*. Another common acronym for nitroguanidine used both in the English and German is *„NGu"* [11,12]. In wartime Germany *„G-Salz"* was used as a disguise for NGu and nowadays *„Nigu"* is another common acronym used in Germany. However, the latter may be confused with the leading manufacturers name (NIGU Chemie GmbH). In the context of this paper we will solely refer to nitroguanidine as

[a] *E.-C. Koch*
Lutradyn – Energetic Materials
Burgherrenstrasse 132, D-67661 Kaiserslautern, Germany
**e-mail: e-c.koch@lutradyn.com*
Homepage: www.lutradyn.com

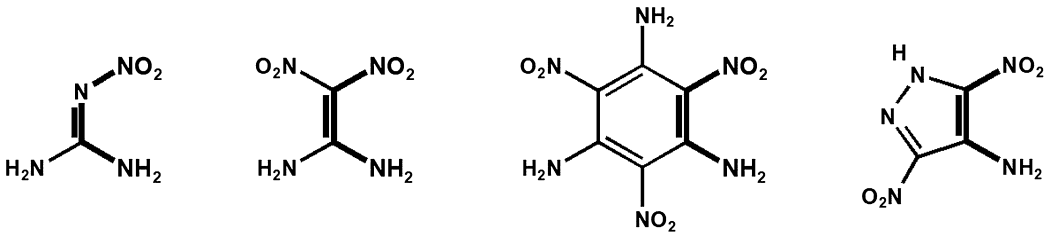

2 3 4 5

Figure 2. Emphasized vicinal amino-nitro-arrangement in NGu (**2**), FOX-7 (**3**), TATB (**4**) and LLM-116 (**5**).

NGu (**2**). NGu is characterised by its chemical formula, $CH_4N_4O_2$ and its CAS-No [556–88–7] (though the entry in CAS is linked to the erroneous nitramine – structure **B** as depicted in Figure 2).

NGu is an off-white crystalline material occurring in solid and hollow needles of large l/d ratio, as platelets from crystallisation with colloidal agents and as spherical grains through crystallization from special solvents. Important physical and chemical properties of NGu and of its direct precursor, guanidinium nitrate (**1**), are depicted in Table 1.

3 Producer

In NATO member states the exclusive bulk producer for NGu is *AlzChem Trostberg GmbH* with headquarters in Trostberg, Germany located in the Bavarian Chemical Triangle [15].

4 Synthesis and Formation of Nitroguanidine

The process flow chart for Nitroguanidine production starting from burnt lime stone and coke is depicted in Scheme 2.

4.1 Industrial Process

4.1.1 NGu-Precursor

4.1.1.1 Calcium Carbide – Calcium Cyanamide

The largescale industrial process chain of NGu typically starts with the production of calcium carbide from burnt limestone and carbon according to

$$CaO(s) + 3C(s) + 0.23\,kWh^{-1}\,mol^{-1} \xrightarrow{\text{electrically heated furnance}} CaC_2(l) + CO(g) \quad (1)$$

with an increasing amount of anthracite being nowadays replaced by plastic waste fraction. The reaction of calcium carbide in the presence of catalytic amounts of $CaCl_2$ or CaF_2 with nitrogen yields calcium cyanamide, $CaCN_2$ (*Polzeniusz-Krauß process*).

Table 1. Properties of nitroguanidine (NGu) and its precursor guanidinium nitrate (GuN) after Ref. [7, 13, 14].

	Unit	NGu (**2**)	GuN (**1**)
CAS-No.		[556–88–7]	[506–93–4]
Formula		$CH_4N_4O_2$	$CH_6N_4O_3$
Ω	wt.-%	−30.75	−26.21
N	wt.-%	53.83	45.89
m_r	$g\,mol^{-1}$	104.068	122.084
ρ at 298 K	$g\,cm^{-3}$	1.759	1.444
$\Delta_f H$	$kJ\,mol^{-1}$	−86	−387
Mp	°C	257 (dec.)	217
T_{dec}	°C	254	250
$\Delta_{ex} H$	$kJ\,mol^{-1}$	−405.7	−345.7
	$kJ\,g^{-1}$	−3.898	−2.831
	$kJ\,cm^{-3}$	−6.857	−4.066
c_p	$J\,g^{-1}\,K^{-1}$	1.198	–
c_L	$m\,s^{-1}$	3350*	–
κ	$W\,m^{-1}\,K^{-1}$	$4.1\,10^{-3}$	–
$S(H_2O)$ at 25 °C	$g\,kg^{-1}$	3.45	165
ARC	°C	159, $\phi = 5.82$	–
V_D	$m\,s^{-1}$	8344#	3700 (at 1.436 $g\,cm^{-3}$)
P_{CJ}	GPa	29.0#	
$\sqrt{2E_G}$	$m\,s^{-1}$	2435#	–
Impact	J	> 50	> 50
Friction	N	> 355	> 355

* 95 wt.-% NGu, 5 wt.-% Estane, $\rho = 1.704\,g\,cm^{-3}$ (98. 7% TMD). # 95 wt.-% NGu, 5 wt.-% Viton® A, $\rho = 1.742\,g\,cm^{-3}$ (97.9% TMD). *Index:* ARC = Adiabatic self-heating onset temperature (°C); CAS = Chemical Abstracts Service Registry Number; c_L = Velocity of sound (longitudinal) ($m\,s^{-1}$); c_p = Specific heat ($J\,g^{-1}\,K^{-1}$); Friction = Friction Sensitivity with BAM-apparatus; GuN = Guandine nitrate, $CH_6N_4O_3$; Impact = Impact Sensitivity with BAM-apparatus; Mp = Melting point (°C); m_r = Molecular mass ($g\,mol^{-1}$); P_{CJ} = Detonation (Chapman Jouguet) Pressure (GPa); S = Solubility ($g\,kg^{-1}$); T_{dec} = Decomposition temperature (°C); T_i = Ignition temperature (°C); $\Delta_{ex} H$ = Enthalpy of explosion ($kJ\,mol^{-1}$); $\Delta_f H$ = Enthalpy of formation ($kJ\,mol^{-1}$); κ = Thermal conductivity ($W\,m^{-1}\,K^{-1}$); Ω = Oxygen balance (wt.-%), N = Nitrogen Content (wt.-%); ρ = Density ($g\,cm^{-3}$); $\sqrt{2E_G}$ = Gurney Velocity ($m\,s^{-1}$)

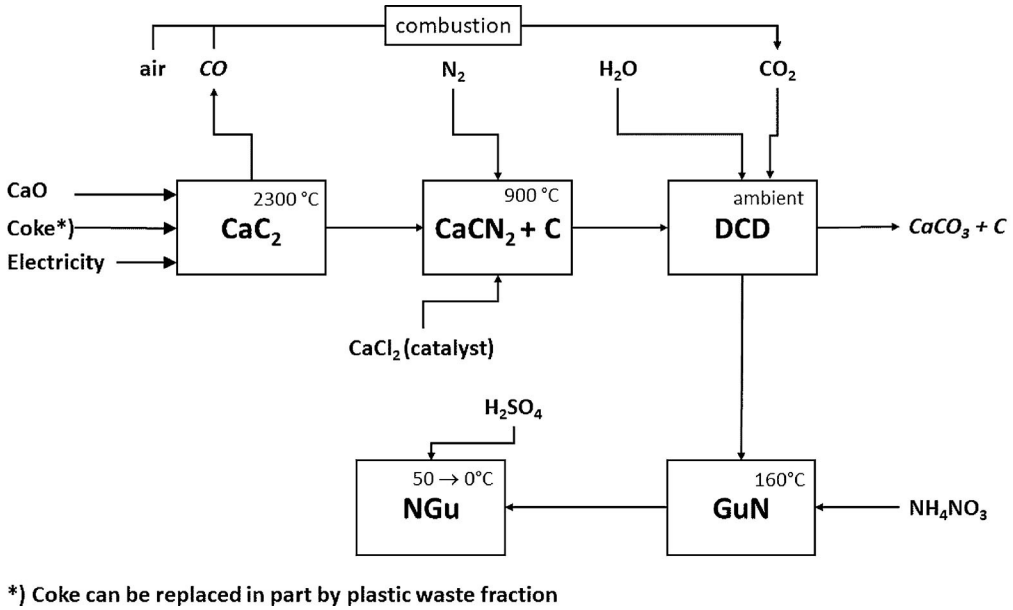

Scheme 2. Flow chart for state-of-the-art Nitroguanidine production.

$$CaC_2(s) + N_2(g) \xrightarrow{700-900^\circ C,\ CaX_2} CaCN_2(s) + C(s) + 286\,kJ\,mol^{-1} \quad (2)$$

The alternative *Frank-Caro process* operates at higher temperature and requires initial ignition of a reaction mixture diluted with ~20 wt.-% $CaCN_2$.

4.1.1.2 Dicyandiamide

Calcium cyanamide is hydrolysed in cold water to yield dicyandiamide (DCD)(**6**) (Figure 3) in a two-step reaction:

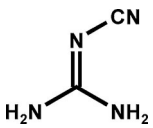

Figure 3. Structure of dicyandiamide, (**6**).

$$2CaCN_2(s) + 2H_2O(l) \rightarrow Ca(CN_2H)_2(s) + Ca(OH)_2(s) \quad (3a)$$

$$Ca(CN_2H)_2 + 2H_2O(l) \rightarrow Ca(OH)_2 + (H_2N)_2C{=}N{-}C{\equiv}N\ [16] \quad (3b)$$

Important properties of DCD are given in Table 2.

Table 2. Properties of dicyandiamide, DCD (**6**).

	Unit	
CAS-No.		461-58-5
Formula		$C_2H_4N_4$
Ω	wt.-%	−114.17
N	wt.-%	66.64
m_r	$g\,mol^{-1}$	84.081
ρ at 298 K	$g\,cm^{-3}$	1.404
$\Delta_f H$	$kJ\,mol^{-1}$	+23
c_p	$Jg^{-1}K^{-1}$	1,415
$S(H_2O)$ at 20 °C	$g\,kg^{-1}$	32
Mp	°C	211
T_{dec}	°C	252

Abbreviations: CAS = Chemical Abstracts Service; c_p = Specific heat ($J\,g^{-1}K^{-1}$); Mp = Melting point (°C); m_r = Molecular mass ($g\,mol^{-1}$); *S* = Solubility ($g\,kg^{-1}$); T_{dec} = Decomposition temperature (°C); $\Delta_f H$ = Enthalpy of formation ($kJ\,mol^{-1}$); Ω = Oxygen balance (wt.-%), *N* = Nitrogen Content (wt.-%); ρ = Density ($g\,cm^{-3}$);

4.1.1.3 Guanidinium Nitrate

There are around twenty different routes for the synthesis of GuN. In the following only those relevant on a technical scale will be discussed.

4.1.1.3.1 Guanidinium Nitrate from Ammonium Thiocyanate

Ammonium thiocyanate, NH_4SCN, (CAS-No. [172–95–41]) was long a very abundant chemical resulting from the desulphurization of coal gas in municipal gas works with ammonia. Disproportionation of NH_4SCN (eq. 4) yields guani-

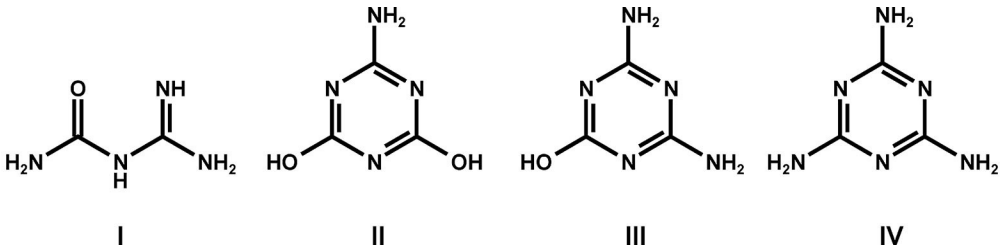

Figure 4. Structural formulas of guanylurea (**I**), ammeline (**III**), ammelide (**II**) and melamine (**IV**).

dine thiocyanate (CAS-No. [593-84-0]) and hydrogen sulphide and has long been a source of guanidine. However, yields are $< 40\,\%$.

$$2NH_4SCN \rightarrow [(NH_2)_3C][SCN] + H_2S \quad (4)$$

Guanidinium thiocyanate then is converted into GuN following treatment with sulphuric acid and nitric acid [17]. The low yield of eq. 4 prompted *Gockel* to refine the process. Purging ammonia gas over dry ammonium thiocyanate yields a liquid phase which then serves as a reactant and solvent for lead nitrate, $Pb(NO_3)_2$, to form GuN in 70% yield [18, 19] (eq. 5).

$$NH_4SCN + 2NH_3 + Pb(NO_3)_2 \rightarrow GuN + PbS\downarrow + NH_4NO_3 \quad (5)$$

Gockel's process has led to explosions probably due to formation of impact sensitive lead species as is speculated in Ref. [20].

An alternative is the Canadian *Welland Process* (named after the former exclusive NGu production facility Welland Chemical works in Welland, ON, Canada in North America [21]) in which ammonium nitrate replaces lead nitrate in liquified ammonia ($NH_4NO_3 \cdot x\ NH_3$), *Divers'-liquid*, CAS-No: [18303-85-0] [22].

$$NH_4SCN + NH_4NO_3 + NH_3 \leftrightarrow GuN + H_2S + NH_3 \quad (6)$$

Davis asserted that NGu prepared through GuN from ammonium thiocyanate adversely affects the stability of Nitrocellulose due to trace contaminations with sulphur compounds [23, 24]. However, no independent confirmation or details of this mechanism are available.

4.1.1.3.2 Guanidinium Nitrate from DCD

State of the art large scale GuN production proceeds through the reaction of DCD with a twofold molar excess of molten ammonium nitrate (Eq. 7), [25]. To prevent thermal runaway of this exothermic reaction it is typically carried out in the presence of a solvent such as water or liquified ammonia. Yields are typically in excess of 90% with small amounts of unreacted ammonium nitrate. Other typical side products include guanylurea (**I**), ammonia, carbon dioxide and triazine derivatives like ammeline (**III**), ammelide (**II**) and melamine (**IV**)(Figure 4) [26].

$$\begin{gathered}(H_2N)_2C{=}N{-}C{\equiv}N{+} \\ 2NH_4NO_3 \xrightarrow{160^\circ C\ autoclave\ water} 2GuN + 21\ kJ\end{gathered} \quad (7)$$

4.1.1.3.3 Guanidinium Nitrate from $CaCN_2$

Calcium cyanamide can be used to produce GuN directly by reacting it with a surplus of molten ammonium nitrate [27] or ammonium nitrate mixed with additional urea (to lower the melting temperature and scavenge sulphur contaminants) [28]. Guanidinium nitrate (GuN) forms as indicated in eq. (8). However, one nitrate equivalent is converted into calcium nitrate which needs to be recycled.

$$CaCN_2(s) + 3NH_4NO_3(l) \xrightarrow{200-220^\circ C} 2NH_3\uparrow + Ca(NO_3)_2(s) + GuN(s) \quad (8)$$

To prevent thermal runaway, it has been proposed in [29], to prepare an intermediate melt containing H_2O, $CaCN_2$, and NH_4NO_3 in a ratio of 1 : 2 : 14. To this is gradually added $CaCN_2$ while the melt is kept at 97° C (*British Aqueous Fusion (BAF) process*) [30].

4.1.1.3.4 Guanidinium Nitrate from Urea and Ammonium Nitrate/UAN

Boatright, *Mackay* and *Roberts* developed a process (*BMR*) based on the reaction between urea and ammonium nitrate in the presence of silica gel (eq. (9–10)) [31–33].

$$Urea + Silica\ gel \leftrightarrow Si{-}O{-}C(=NH)NH_2 + H_2O \quad (9)$$

$$Si{-}O{-}C(=NH)NH_2 + NH_4NO_3 \leftrightarrow Si{-}OH + GuN \quad (10)$$

The *BMR* process had been intensively studied by the U.S. ARMY in the 1970s when plans were made to install the first ever CONUS-NGu production line in the USA at the Sunflower Army Ammunition Plant (SFAAP) [34]. However, when the NGu production at SFAAP finally started in 1984

Table 3. Nitroguanidinium Salts, $[NGuH]^+[X]^-$.

	Unit	Nitrate	NGuH:GuN	Chloride	Hydrogensulphate	Perchlorate
CAS-No.		98205-29-9	1017262-73-5	65943-79-5	–	15179-01-8
Formula		$C_1H_5N_5O_5$	$C_2H_{11}N_9O_8$	$C_1Cl_1H_5N_4O_2$	$C_1H_6N_4O_6S_1$	$C_1Cl_1H_5N_4O_6$
Ω	wt.-%	4.79	−8.30	−22.77	−7.91	15.65
N	wt.-%	41.917	43.56	39.869	27.717	27.394
m_r	g mol^{-1}	167.081	298.17	140.529	202.147	204.53
ρ at 298 K	g cm^{-3}	1.8	1.706	1.72	–	–
$\Delta_f H$	kJ mol^{-1}	−335	–	–	–	–
Mp	°C	126	–	–	–	–
T_{dec}	°C	147	–	–	–	105

Abbreviations: CAS = Chemical Abstracts Service; Mp = Melting point (°C); m_r = Molecular mass (g mol^{-1}); T_{dec} = Decomposition temperature (°C); $\Delta_f H$ = Enthalpy of formation (kJ mol^{-1}); Ω = Oxygen balance (wt.-%), N = Nitrogen Content (wt.-%); ρ = Density (g cm^{-3});

the *BAF* process (starting with calcium carbide) had been put in place instead [35].

4.2 Nitroguanidine

4.2.1 Nitration of Guanidinium Nitrate (GuN)

4.2.1.1 Nitration of GuN with Sulphuric Acid and Mixed Acid

For convenience we will use the following non-IUPAC abbreviations in the further discussion:

- Gu = Guanidine, $HN{=}C(NH_2)_2$
- GuH^+ = Guanidinium, $[C(NH_2)_3]^+$
- NGu = Nitroguanidine, $O_2N{-}N{=}C(NH_2)_2$
- $NGuH^+$ = Nitroguanidinium, $[(O_2N{-}NH)C(NH_2)_2]^+$

NGu is formed upon reaction of GuN with concentrated sulphuric acid according to Scheme 1 in yields > 90 %. However, the reaction is not a dehydration, but a complex sequence of steps starting with the formation of the actual nitrating species, the nitronium cation, NO_2^+, according to Eqs. 11–12.

$$GuH^+ + NO_3^- + H_2SO_4 \leftrightarrow GuH^+ + HNO_3 + HSO_4^- \quad (11)$$

$$HNO_3 + 2H_2SO_4 \leftrightarrow NO_2^+ + H_3O^+ + 2HSO_4^- \quad (12)$$

As a base (*though weak pK_b(NGu) = 12.4* [36] *when compared to guanidine, pK_b(Gu) = 13.6*) nitroguanidine dissolves in concentrated strong acids to form the corresponding nitroguanidinium salts which in some cases can be isolated as crystalline substances (chloride [37], hydrogensulphate [38, 39], nitrate [37], perchlorate [40], see Table 3) directly from the acidic solutions (Eq. 13). A (1 : 1) double salt of the nitroguanidinium nitrate with guanidinium nitrate has been characterized by *Klapötke et al.* [41].

$$NGu + HX \leftrightarrow NGuH^+ + X^- \quad (13)$$

However in more dilute solutions (e.g. < 20 wt.-% H_2SO_4) and with excess water the nitroguanidinium salts decompose to give the conjugate base, nitroguanidine, which then precipitates due to its low solubility in water (3.45 g l^{-1} at 298 K), (Eq. 14) (see Figures 5–7) [42].

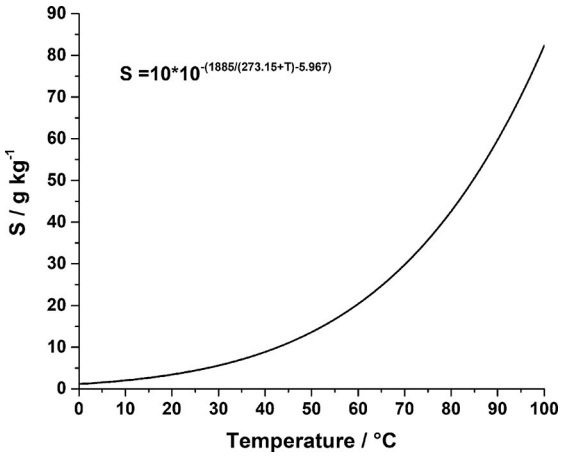

Figure 5. Solubility of NGu in water after Ref. [43].

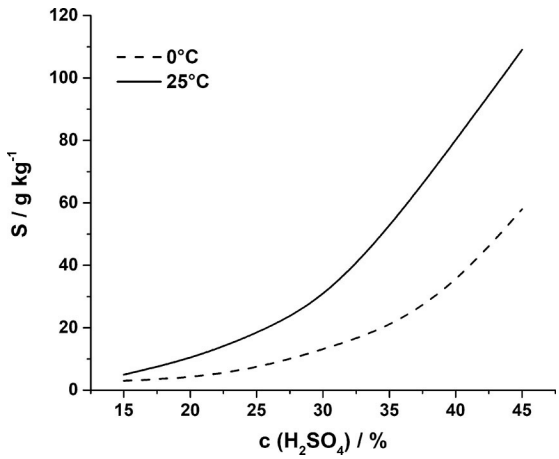

Figure 6. Solubility of NGu in sulphuric acid after Ref. [44].

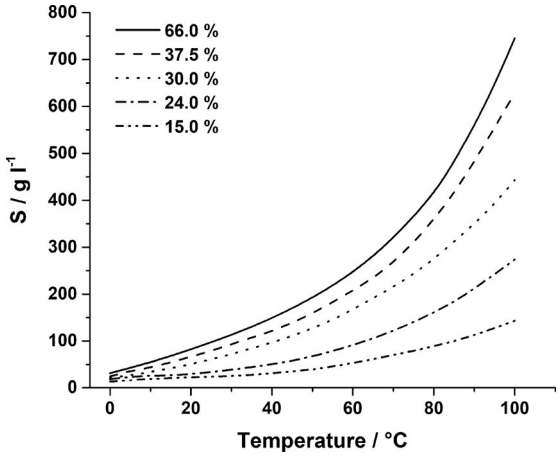

Figure 7. Solubility of NGu in nitric acid of different concentrations as function of temperature after Ref. [45].

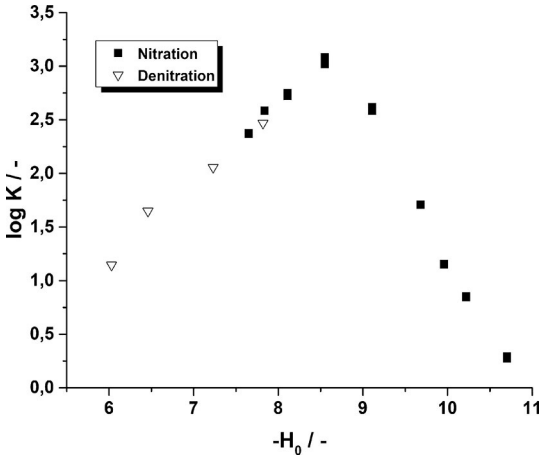

Figure 8. Equilibrium product, log K versus Hammett acidity function for H_2SO_4 for eq. 12 after ref. [38].

$$NGuH^+ + X^- + H_2O \leftrightarrow NGu \downarrow + H_3O^+ + X^- \quad (14)$$

The NGu-formation proceeds through *N*-nitration of the guanidinium ion (eq. 15). This is the rate determining step. The nitration depends on the concentration of both guanidine and HNO_3 and follows a second order kinetics [38,46].

$$GuH^+ + NO_2{}^+ \leftrightarrow NGuH^+ + H^+ \quad (15)$$

The underlying equilibrium reads

$$K = [NGuH^+] \cdot [H_2SO_4]/[GuH^+] \cdot [NO_2{}^+] \cdot [HSO_4{}^-]$$

The nitration is a reversible process and hence solutions of NGu in sulphuric acid and other strong acids may serve as nitrating reagent for various substrates [47,48]. The denitration in concentrated sulphuric acid follows a first order kinetics, based on the c(NGu) [49,50].

$$NGuH^+ + H^+ \leftrightarrow GuH^+ + NO_2{}^+ \quad (16)$$

Figure 8 depicts the relationship between Hammett acidity function, $-H_0$ for sulphuric acid and log K for both denitration (open triangles) and nitration (filled squares) and shows the optimum concentration for conversion of GuN into NGu at c: $-H_0 = 8{,}5 \sim 88\%$ H_2SO_4 [38] which is similar to the concentration range observed for high-rate reactions in aromatic nitrations [51].

The nitration of GuN in sulphuric acid and mixed acid is conducted at ambient temperatures and typically gives yields in excess of 98% [52]. *Liu et al.* [53] have investigated the kinetics of the N-nitration of GuN in mixed acid H_2SO_4/HNO_3/H_2O (81/5/14) and confirmed the reaction to follow a second order kinetics.

4.2.1.2 Nitration of GuN with Nitric Acid

Schirra et al. have developed a process for technical scale production of NGu by nitration of GuN with highly concentrated HNO_3 and subsequent hydrolysis of the nitroguandinium nitrate [54,55]. According to *Astrat'ev et al.* [56] the nitration of GuN in nitric acid at concentrations c = (HNO_3) 82–92% follows a second order kinetics. However above c(HNO_3) > 90% dinitroguanidine forms in 20–25% yield. Hence NGu synthesis must occur at lower c(HNO_3) but also sufficient temperature to proceed at reasonable speed. Again, temperatures must not exceed T = 60–70 °C to avoid decomposition of NGu. The addition of 1.5 wt.-% sodium nitrite, $NaNO_2$, to 84.6% HNO_3 at T = 25 °C is equivalent a temperature-rise of 50 °C and hence avoids thermal decomposition of NGu to GuN. The temperature sensitivity of NGu formation from GuN in nitric acid has been investigated by *Kang et al.* [57]. Technical yields for NGu obtained from nitration of GuN with HNO_3 typically range between 80–85%.

4.2.2 Nitration of Dicyandiamide

Marqueyrol & Loriette proposed to synthesise NGu starting directly from DCD [58]. The process starts with the reaction of DCD with sulphuric acid to give guanidinium sulphate and the reaction of latter with mixed acid to give NGu. The overall yield is 0.83 mol NGu per mol DCD. A process avoiding the use of sulphuric acid has been suggested by *Mayer* [59]. Therefore, ammonium nitrate and excess nitric acid are reacted to form ammonium trinitrate $NH_4NO_3 \cdot 2HNO_3$ [60]. To this mixture is added DCD. After heating to T = 60–70 °C intense gas evolution is indicative of an exothermic process that needs to be controlled by cooling. Finally, the mixture is cooled to ambient temperature neutralised with ammonia whereupon NGu starts to precipitate. The AN solution is recycled in the process to form new ammonium trinitrate.

Astrat'ev et al. [56] also studied the nitration of DCD. They observed the formation of nitroguanylurea which under the reaction conditions decomposes to guanyl isocyanate and nitramide. Nucleophilic decomposition of guanyl isocyanate to guanidinium and successive nitration complete the process. However, the yield is 0.5 mol at best per mole DCD applied [22] and a disproportionally large amounts of nitric acid is required to conduct the process.

4.2.3 Alternative Routes

Aside from the direct nitration of guanidine NGu should be accessible through procedures typically used for *N*-nitroimines [61].

4.2.3.1 Urea as Starting Material

Under the false assumption that NGu is a nitro-amine (structure **B** in Figure 1), *Watt & Maskosky* unsuccessfully tried to prepare NGu by reaction of nitrourea with liquid ammonia in accordance with eq. (17) [62].

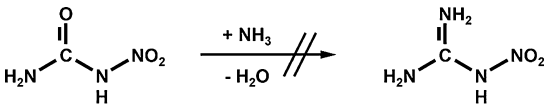

(17)

2 B

However instead the formation of nitramide, NH_2NO_2, and urea is observed (eq. 18) which also rules out any potential NGu-formation according to eq. 19 which is a typical nitrimine formation process for carbonyl compounds [61].

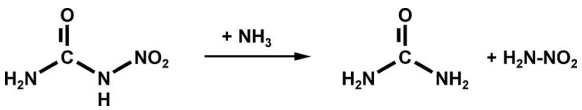

(18)

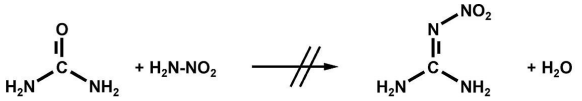

(19)

2

4.2.3.2 Nitrosation of N-Hydroxyguanidin

Oximes (**V**) can be used to prepare nitrimines (**VII**) [61] according to the general sequence in eq. 20.

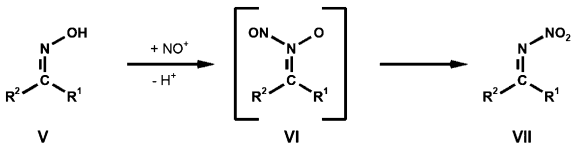

(20)

V **VI** **VII**

This reaction proceeds smoothly with a great variety of substrates mostly with bulky alkyl and cycloalkyl substituents, R^1 and R^2. In contrast with hydroxyguanidines of the type (**Va**) with R=H [63], *p*-nitrotolyl, *p*-mesityl etc. the reaction stops with the formation of stable diazeniumdiolates **VIa** which can be isolated and have been structurally characterised [64]. Hydroxyguanidine reportedly undergoes the same reaction to give **VIa** (CAS-No. [1314899-37-0]) with R=H which is an isomer of NGu. However, no rearrangement of VIa to NGu has been observed in Ref. [64]. **VIa** and its derivatives are considered as potential NO-donors in biological systems [65].

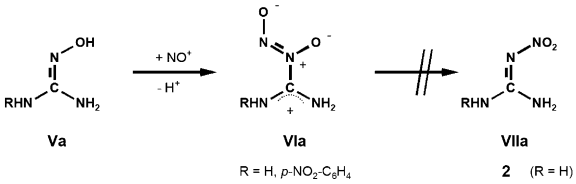

(21)

Va **VIa** **VIIa**

R = H, *p*-NO_2-C_6H_4 **2** (R = H)

5 Crystallography

5.1 Crystal Habit and Particle Morphology

5.1.1 Crystals from Aqueous Solutions Without Additives

Nitroguanidine crystallizes from acidic solutions as orthorhombic needles, space group: *Fdd2*. The sometimes hollow needles have a large length to diameter (*l/d*) ratio. This crystal habit of NGu is often referred to as „α-nitroguanidine" [66]. Figure 9 shows an optical micrograph of such crystals with a *Fisher Sub Siever Size* (FSSS): 2.7 μm. If NGu is allowed to crystallize for a longer time then thick needles (FSSS: 6.6 μm) are obtained as is indicated in Figure 10.

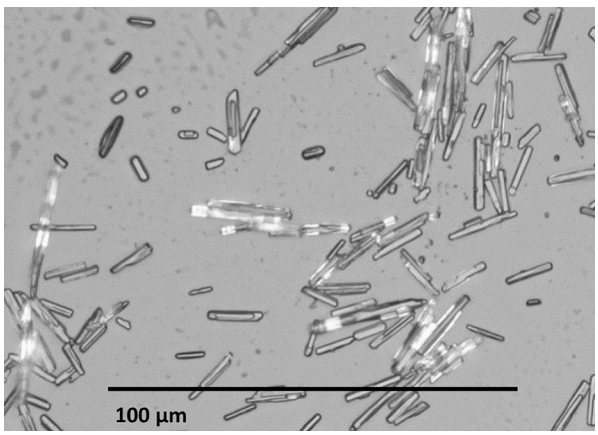

Figure 9. Optical Micrograph of LBD-NGu (as is) (*courtesy of Alz-Chem Trostberg GmbH*).

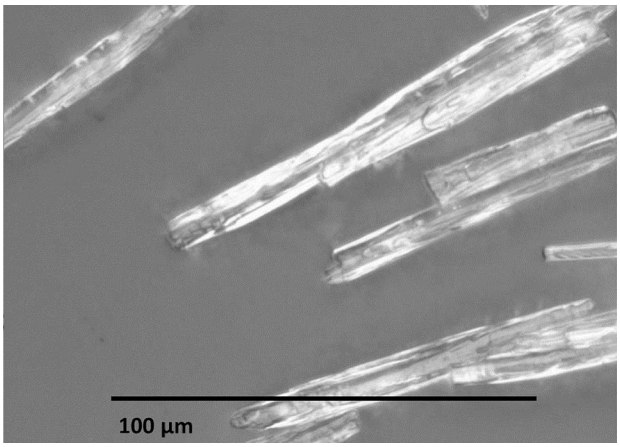

Figure 10. Optical Micrograph of LBD-NGu (grown) (*courtesy of Alz-Chem Trostberg GmbH*).

Figure 11 shows an electron micrograph of LBD-NGu. Random lateral contact of NGu crystals along their {110} or {010} faces (Figure 12) yields linear bundles, tubes and step-like crystals.

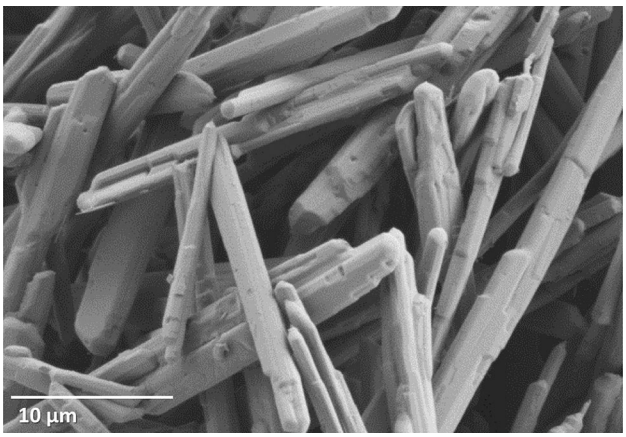

Figure 11. Electron Micrograph of LBD-NGu (as is) (*courtesy of Alz-Chem Trostberg GmbH*).

Chen et al. [67] simulated the growth of NGu crystals in vacuum and found that the terminal faces correspond to the strong interlayer bonds that are also responsible for the crossing layer stacks as determined by *Zhang et al.* [68]. The predicted crystal habit for NGu grown in vacuum is shown in Figure 13. The {111}-, {131}- and {311}-faces of NGu in vacuum are predicted to grow about three times as fast as the lateral faces {220} and {040} (Table 4). A similar needle crystal habit (among other habits) is obtained with 1,3-diamino-2,4,6-trinitrobenzene (DATB) [69] which also forms strong interlayer bonds and has the same crossing layers as NGu [68].

Table 4. Crystal habit parameters for NGu in vacuum after Ref. [67].

{*hkl*}	Unit	{220}	{040}	{111}	{131}	{311}
$d_{hkl}^{(a)}$	pm	727	646	381	352	325
$E_{att}^{(b)}$	kJ mol^{-1}	−273.68	−408.57	−820.15	−819.44	−768.48
$R^{(c)}$	–	1	1.49	3.00	2.99	2.81

a) interplanar distance, b) face attraction energy, c) relative growth velocity

Evaporation of hot NGu solutions in high vacuum yields fine short needles which can be better consolidated than the long needles and have an even greater surface area [11]. Ultra-fine NGu particles have been obtained from treatment of LBD-NGu in an attrition mill [70]. While for propellant applications a needle type material is advantageous as it lends both mechanical reinforcement of the propellant grain and high surface area which is necessary to allow for fast combustion it is not suitable for highly dense high explosive formulations. At first needle type crystals do not pack very well which hampers consolidation, secondly the cavities in hollow needles remain inaccessible to binder and hence impede to attain a sufficient density. Finally, the high surface area of LBD-NGu dramatically alters the viscosity of both melt-cast and cure cast formulations and thus impedes to obtain high solid loadings.

5.1.2 Colloidal Agents as Crystal Habit Modifiers

Research into crystal habits allowing for a higher bulk density was first conducted in wartime Germany. Then crystallization of hot ($T > 80\,^{\circ}C$) aqueous solutions of NGu (pH = 7) modified with colloidal agents such as polyvinylalcohol [9002–89–5] and hydroxyethylmethylcellulose [9032–42–2] gave a high bulk density NGu with $\rho > 1.0$ which was then used in highly insensitive melt-pour TNT/NGu formulations for use in armour piercing ammunition [11, 72, 73]. However, those findings were not patented until after the war [74]. A modified process is described in [75]. Yet another similar process using PVA and methylcellulose [9004–67–5] as colloidal agents has been described yielding HBD-NGu with jagged granular and ovate crystal habit and bulk densities up to $\rho \sim 1.0\ g\,cm^{-3}$ [76, 77]. A study of process parameters on the production of HBD-NGu has been done by *Mudryy et al.* [78]. The effect of various modifiers on the crystallization process and obtained habit of NGu has been investigated by *Gong et al.* [79]. They find that hydroxyethylcellulose [9004-62-0] yields hexagonal shaped platelets which result in superior bulk density when compared with prior art additives. *Kohlbeck* found that cyclic amine impurities (presumably compounds **II**, **III** and **IV**), carried through the process chain, affect the crystal habit accessible in HBD-NGu recrystallisation [80].

Figures 14 and 15 depict the rhombohedral morphology of high bulk density NGu prepared by crystallization of NGu

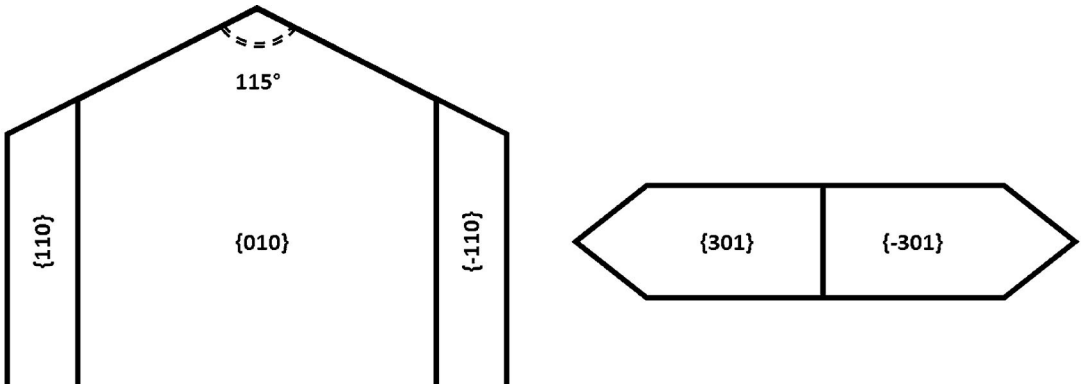

Figure 12. Face and side view of NGu crystal morphology and *hkl* indices for α-Nitroguanidine grown from aqueous solutions after Ref. [71].

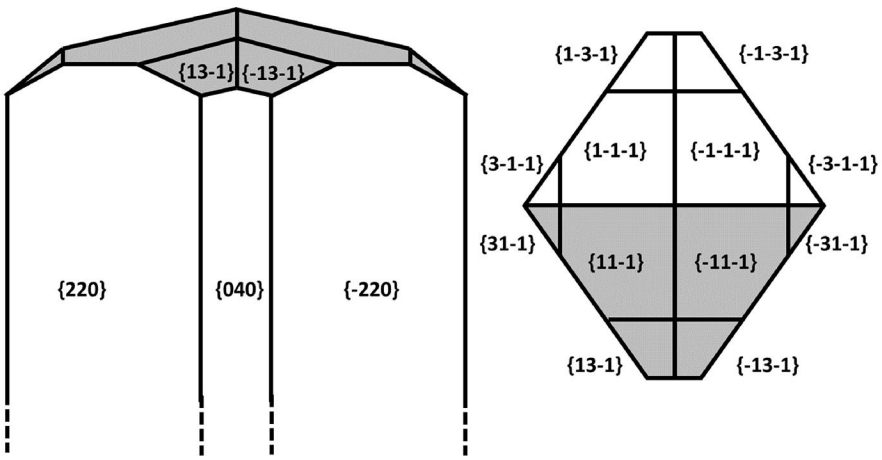

Figure 13. Face and side view of calculated NGu crystal morphology and *hkl*-indices for α-Nitroguanidine grown in vacuum after Ref. [66].

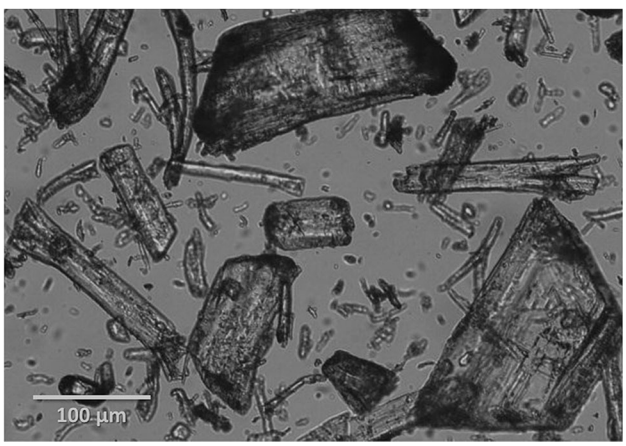

Figure 14. Optical Micrograph of HBD-NGu (*courtesy of AlzChem Trostberg GmbH*).

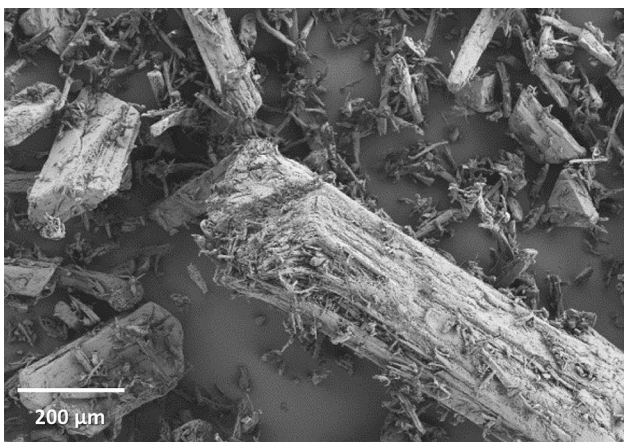

Figure 15. Electron Micrograph of HBD-NGu (*courtesy of AlzChem Trostberg GmbH*).

from aqueous solutions modified with proprietary colloidal agents at *NIGU Chemie* Germany.

5.1.3 Crystals from Organic Solvents

Nitroguanidine dissolves best in aprotic polar solvents. In protic solvents sparing solubility is observed. Aprotic non-polar solvents such as benzene, chloroform, carbon disulphide, tetrachloromethane and toluene do not dissolve NGu [81] which is also in line with the observation that NGu is insoluble in supercritical CO_2 [82]. Table 5 shows solubility of NGu in different solvents.

Table 5. Solubility of Nitroguanidine in selected solvents in increasing order of solubility (at 19–20 °C) for reported temperatures.

Solvent	Solubility ($g\,kg^{-1}$ Solvent)	Temperature (°C)	Ref.
diethyl ether	0.40	19	[81]
ethyl acetate	0.50	19	[81]
ethanol, 100 Vol-%	1.22	19	[81]
ethanol, 96 Vol-%	1.66	19	[81]
	1.80	20	[44]
acetone	1.90	20	[44]
	2.67	20	[81]
methanol	3.02	19	[81]
	5.0	20	[44]
ethylene glycol (EG)	11.0	20	[83]
	90	100	[84]
pyridine	17.5	20	[82]
dimethylformamide (DMF)	120	20	[83]
	150	25	[85]
	200	60	[85]
	265	80	[85]
	280	98	[85]
N-methyl-2-pyrrolidone (NMP)	159*	25	[86]
dimethyl sulphoxide (DMSO)	~100	20	
glycerol/water (1:1)	70	100	[84]
2, 4-dinitroanisole (2,4-DNAN)	4.48	100	[87]

*) $S(NMP) = 4.3039 + 0.5244 \cdot T - 0.0025 \cdot T^2$ ($T = 20–90$ °C) [g 100 g^{-1} Solvent]

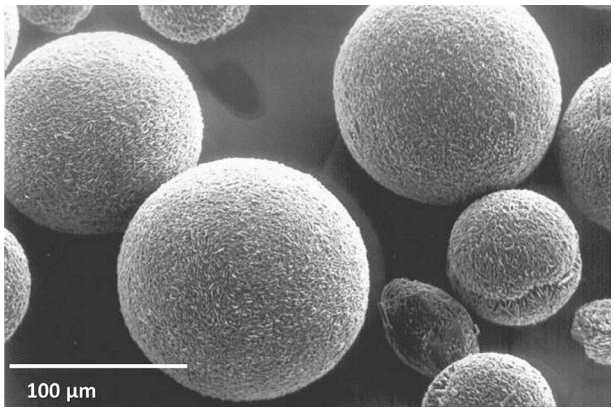

Figure 16. Electron Micrograph of spherulitic NGu (*courtesy of Alz-Chem Trostberg GmbH*).

The enthalpies of dissolution of both DMF and DMSO have been determined in Ref. [88].

Wright observed regular prismatic NGu-crystals from organic solvents [89]. Purging hot saturated aqueous solutions of NGu into equal volumes of those non-solvents (e.g. cold methanol) yields uniform rounded rhombohedral prisms with a bulk density of $\rho = 0.98\ g\,cm^{-3}$ [89]. *Engel* and *Heinisch* further refined this solvent/non-solvent procedure and were able to determine process parameters (cooling profiles) allowing for the technical scale preparation of spheroidal cauliflower-type NGu crystals with high bulk densities even exceeding $1\ g\,cm^{-3}$ (Figures 16, 17) [84, 90]. *Spear et al.* did an extensive parametric study of the recrystallization of NGu from various solvent/non-solvent systems [91] (see Table 6). Spherulitic NGu with $\rho = 1.08\ g\,cm^{-3}$, is accessible by the solvent/non-solvent method using NMP/acetone and nickel nitrate as an additive in solvent [92, 93]. A more recent study of solvent/non-solvent (NMP/acetone) crystallisation was conducted by *Lu et al.* [86].

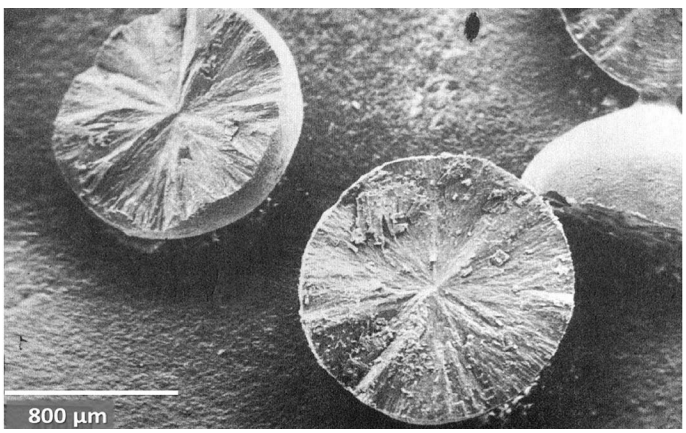

Figure 17. Electron Micrograph of Spherulitic NGu cross section (from Ref. 84).

Table 6. Selected experimental results from solvent/non-solvent combinations.

Solvent	Non-solvent	ρ_{bulk} (g cm^{-3})	Morphology	Yield (%)	Ref.
glycerol/water (50:50)	2-propanol	0.94	spheroidal	77	[84]
EG	acetone (A)	1.02	spheroidal	84	[84]
NMP	A	*	*		[91]
DMSO	A		needles		[91]
EG/DMSO	A/ethanol		no crystallisation		[91]
DMF	A		needles/raspberries		[91]
DMF/DMSO	A		needles		[91]
EG	A		needles		[91]
pyridine/NMP	A		rough spheres		[91]

* Depending on process parameters (time, concentration, temperature) a range of small to large spheroidal crystals with varying bulk densities could be obtained

Yet another process to HBD-NGu was achieved by *Heinisch, Hommel* and *Thiel* [94–96]. They devised minute parameters for the cooling of saturated DMF and NMP solutions to obtain high bulk density spherulitic NGu. *Maranda & Orzechowski et al.* found compact prisms upon crystallisation of NGu from ethylene glycol and nice spherulitic grains from NMP [83, 97] (Figures 18, 19).

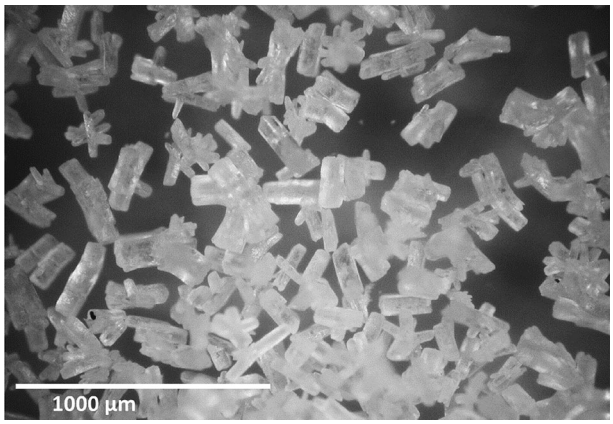

Figure 18. Optical Micrograph of prismatic NGu recrystallized from ethylene glycol (*reproduced with kind permission by Prof A. Maranda*).

NGu has been specified with regards to chemical composition, particle size and specific surface area for military applications at NATO level [98]. The US legacy standard MIL-N-494 A has been reactivated as of August 8 2013 [99]. The corresponding UK specification, DEF-STAN 07-012/1 has been withdrawn on March 31 2014 [100].

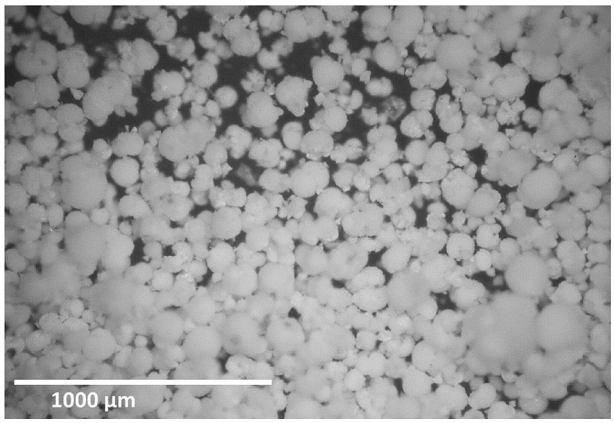

Figure 19. Optical Micrograph of spherulitic NGu recrystallized from DMF (*reproduced with kind permission by Prof A. Maranda*).

Table 7 compares the salient properties of UF-, LBD-, HBD- and SHBD-NGu and their most common uses.

Table 7. Properties of different NGu particle morphologies.

	units	UF	LBD	HBD	SHBD
ρ_{cryst}	g cm^{-3}		1.72–1.73	1.75	1.76
ρ_{bulk}	g cm^{-3}		0.3	0.9	1.15
A_s	m^2 g^{-1}	>100	4–25	4	<0.5
Crystallite size	nm		~120	~120	
Morphology	–	granular	needles	platelets, prisms	spheroids
Diameter	µm	0.300	3–15	60–70	50–1000
Uses[a)]	–	GP	GP	RP, HE	HE

a) GP = gun propellants, RP = rocket propellants, HE = high explosives

5.2 Diffractometry

5.2.1 Powder Diffractometry

Bridgman reported about an ill-characterised high-pressure phase transition of NGu close to $p = 3.9$ GPa [101]. At ambient temperature and pressure there is only one crystal phase. This is confirmed by all the published diffraction data for NGu [71, 102–105]. Despite different crystal habits – which have been tentatively assigned α- and β-Nitroguanidine – the underlying crystal lattice of all investigated crystals is *orthorhombic* and space group: *Fdd2*. Table 8 shows the determined cell parameters and the derived density at ambient temperature for different determinations based on 16 formula units NGu in the unit cell.

The lines and intensities are given below in Table 9. Figure 20 depicts the powder diffractogram of a commercial

Table 8. Unit cell dimensions and calculated density of NGu.

Ref.		[71]	[103]	[105]
a	Å	17.47	17.58	17.59
b	Å	24.50	24.84	24.81
c	Å	3.59	3.58	3.589
ρ_{calc}	g cm^{-3}	1.799	1.769	1.765

Table 9. Powder diffraction data after Ref. [105].

2θ (°)	d (Å)	I (-)	2θ (°)	d (Å)	I/(-)
12.40	7.14	2	42.42	2.131	12
14.34	6.18	1	43.66	2.073	6
17.48	5.073	100	44.17	2.050	4
20.22	4.392	9	44.98	2.015	20
21.44	4.144	50	45.37	1.999	4
24.83	3.586	35	47.80	1.903	2
27.54	3.239	14	48.61	1.873	1
28.83	3.097	10	49.03	1.858	3
30.56	2.925	25	50.80	1.797	7
31.16	2.870	10	51.26	1.782	3
33.80	2.652	25	52.53	1.742	2
34.41	2.606	14	54.62	1.680	5
35.99	2.495	13	55.77	1.648	1
37.59	2.392	25	56.76	1.622	5
38.87	2.317	3	59.56	1.552	1
40.26	2.240	1	60.47	1.531	1
41.70	2.166	1	60.92	1.521	1

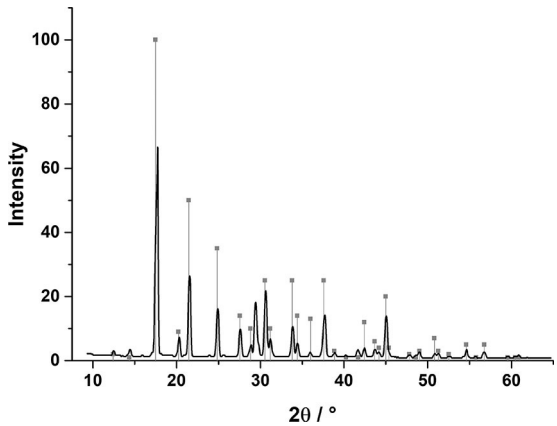

Figure 20. Powder diffractogram of a commercial LBD-NGu sample and reflexes from *Vasil'ev* [105].

LBD-NGu sample and the latest indices from *Vasil'ev* [105] as grey anchor lines.

5.2.2 Crystal & Molecular Structure

The molecular structure of nitroguanidine has long been the subject of intense debate. Apart from theoretical studies and those addressing its chemical reactivity a number of crystallographic studies have been conducted to solve the conundrum whether NGu has a nitrimine or a nitramine structure (Tables 10, 11). Figure 21 depicts a capped stick model of NGu derived from crystallographic data in [6] bearing the designations of all atoms in NGu. Table 10 depicts the bond lengths and angles determined. Figure 22 is a view along the *b*-axis of the cell through the *ac*-plane indicating the so called „crossing-pattern" [68]. The NGu crystal is formed from staggered layers of ribbons of NGu molecules pointing in an alternating fashion left and right with regards to a geometrical axis along N1···N3. These stratified layers of ribbons form an angle of$\angle = 124.07^{\circ}$ with each adjacent layer to yield the pattern depicted in Figure 22.

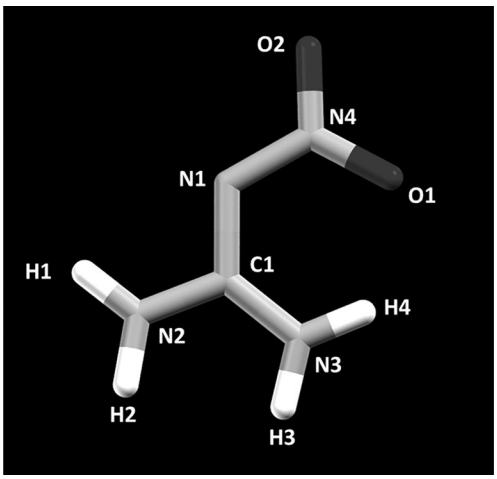

Figure 21. Crystallographic designation of atoms in NGu.

The closest intermolecular distance is observed within each ribbon between H2···O2′(205 pm). The second next close distance is observed at the intersection between those stratified layers between H1···O2″(244 pm). Finally, H2···O2‴: between different layers is ~319 pm.

The position of the hydrogen atoms in NGu has been unambiguously located by *Choi* using neutron diffraction on N2 and N3 [6] proving that NGu is <u>not</u> a nitramine. The N–H bonds are a little shorter than usual Nsp^3–H bonds (96 and 98 pm versus 101 pm) [106].

The intramolecular hydrogen bond O1···H4 is 192 pm which is very similar to FOX-7 (**3**) where the intramolecular hydrogen bond length is 189 nm [107]. The C1–N1 bond length has been determined to d_{C1-N1}: 137.4 pm. However typical double bonds of the type Csp^2=N(2) range between 127–132 pm and the observed value better fit a Csp^2–N(2) d ~ 137 pm. Likewise the expected single bonds C1–N2 and C1–N3 are too short with $d_{C1-N2/3}$: 131.6/132.5 pm respectively. Typical values should range in the 141 pm-ballpark. Finally, d_{N1-N4}: 133.1 is a little too short for an anticipated single bond in the 135 pm range.

Table 10. Crystallographic data of NGu.

	Unit/Ref	[116]	[6]	[117]	[118, 119]	[120]
CCDC-#		1223552	1223553	n.a.	1223554	185118
Density	g cm^{-3}	1.770	1.760	1.816	1.736	1.759(2)
Temperature	K	298	298	113.15	298	293.2
Radiation		CuKα	Neutrons	MoKα	MoKα	CuKα
Crystal system	–	orthorhombic	orthorhombic	orthorhombic	orthorhombic	orthorhombic
Space group	–	Fdd2(43)	Fdd2(43)	Fdd2(43)	Fdd2(43)	Fdd2(43)
Z	–	16	16	16	16	16
a	Å	17.58(9)	17.6152(2)	17.5671(26)	17.6390(5)	17.6181(14)
b	Å	24.82(12)	24.8502(7)	24.8511(48)	24.8730(7)	24.848(2)
c	Å	3.58(2)	3.5880(1)	3.4880(9)	3.5903(1)	3.5901(4)
V	Å^3	1562.08	1570.62	1522,73	1575.19	1571.7(3)

Table 11. Selected bond lengths (pm), bond angles (°) and intramolecular distances (pm) of NGu.

	[116]	[6]	[117]	[118, 119]	[120]
C1–N1	135(2)	135.9(9)	137.0	137.2(3)	137.4(2)
C1–N2	134(1)	133.0(8)	132.9	132.2(2)	131.6(4)
C1–N3	134(2)	130.9(7)	132.6	132.1(2)	132.5(2)
N1–N4	135(2)	135.4(6)	133.1	133.49	133.1(2)
N4–O1	122(2)	126.1(8)	125.4	124.7(2)	123.7(3)
N4–O2	123(2)	122.7(9)	124.0	123.8(2)	124.3(2)
N2–H1	–	96(2)	–	–	
N2–H2	–	100(2)	–	–	
N3–H3	–	98(2)	–	–	
N3–H4	–	96(2)	–	–	
O1–N4–O2	121	120.0(7)	120.1	120.1(1)	120.0(1)
O1–N4–N1	124	122.6(6)	124.2	124.6(1)	124.5(7)
N4–N1–C1	118	119.5(6)	119.4	118.9(5)	118.7(2)
N1–C1–N2	112	111.3(6)	113.1	112.8(2)	112.3(2)
N1–C1–N3	129	128.5(6)	127.9	127.9(3)	128.3(1)
N2–C1–N3	118	120.1(7)	119.0	119.3(2)	119.4(2)
O1···H4	–	193(2)	–	–	–
O1···N3	257	258.7	300	259.4	259.9

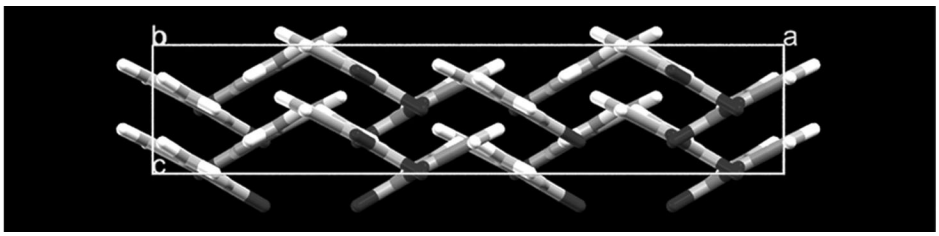

Figure 22. Crossing pattern of Nitroguanidine (view along b axis perpendicular to ac plane).

The crystal structure of the insensitive explosive 1,3,5-triamino-2,4,6-trinitrobenzene (TATB) (**4**) shows extreme long C–C bonds in the ring (d ~ 145 pm) but therefore shortened C–N bonds for the amino (d ~ 131 pm) and (d ~ 141 pm) for the nitro groups [108]. This is interpreted as a push-pull electron delocalisation to iminium nitronate structures (Figure 23 right) which also explain the good stabilisation of the molecule against decomposition [109].

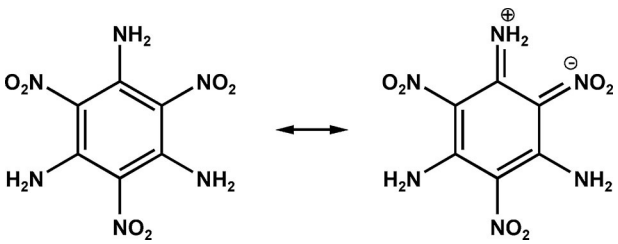

Figure 23. TATB (**4**) and exemplary push-pull delocalisation.

A crystallographic and theoretical analysis of a series of 1,1-diamino-2,2-dinitroethylenes shows a similar situation to persist. The most important member of this the group, the insensitive high explosive FOX-7 (**3**) is also best represented by a zwitterionic structure of the type indicated right in Figure 24 with shorter than normal *d*(C–NH) bonds, 132 pm [110].

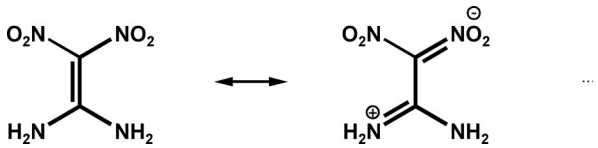

Figure 24. FOX-7 (**3**) and exemplary push-pull delocalisation.

In view of the above the unusual structural features of NGu can be understood too as a push- pull-electron-delocalisation to equivalent iminium nitronate structures as indicated in Figure 25.

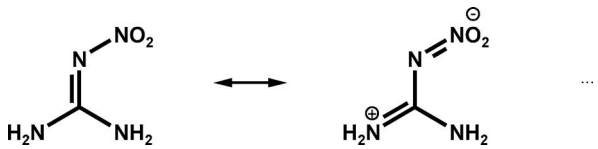

Figure 25. NGu (**2**) and exemplary push-pull delocalisation.

Comparison of NGu with various NGu-derivatives such as dinitroguanidine (**7**) [111], aminonitroguanidine (**8**) [112], diaminonitroguanidine (**9**) [112], *N*-methyl-*N*′-nitroguanidine [113], and 1,1,3,3-tetramethyl-2-nitroguanidine [114] shows that the bond lengths encountered before are not a singularity but common features for nitroguanidines and explain their extraordinary stability and insensitivity by push-pull electron delocalization to iminium nitronate structures (Figure 26).

Crystallographic investigation of a homologous nitroethenediamine derivative reveals the exact same prevalence of a shortened C–NH_2 bonds [115].

5.3 NGu Based Co-Crystals

Co-crystals are crystals having two or more molecules in the same unit cell which do not maintain a covalent bond with each other [121]. Based on thermodynamic parameters (solubility, lattice energy) NGu is predicted to form co-crystals with other energetic materials [122].

Hope & Pulham et al. have prepared co-crystals [123] from NGu and 2-hydroxy-5-nitropyridine, $C_5H_4N_2O_3$, CAS-No: [5418–51–9], in a molar ratio 1 : 1 applying resonant acoustic mixing [124]. Figure 27 displays the diffractogram of the NGu : HNP-co-crystal.

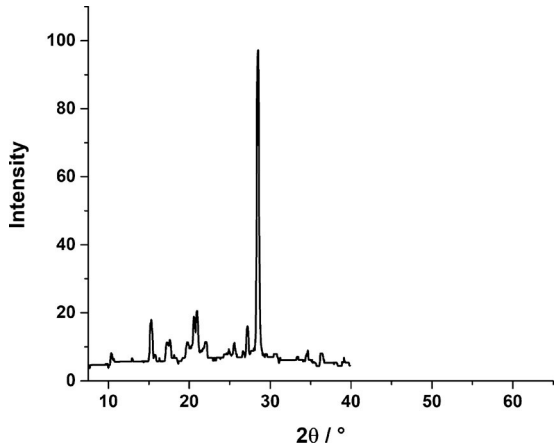

Figure 27. XRD of NGu : HNP co-crystal after data in [124].

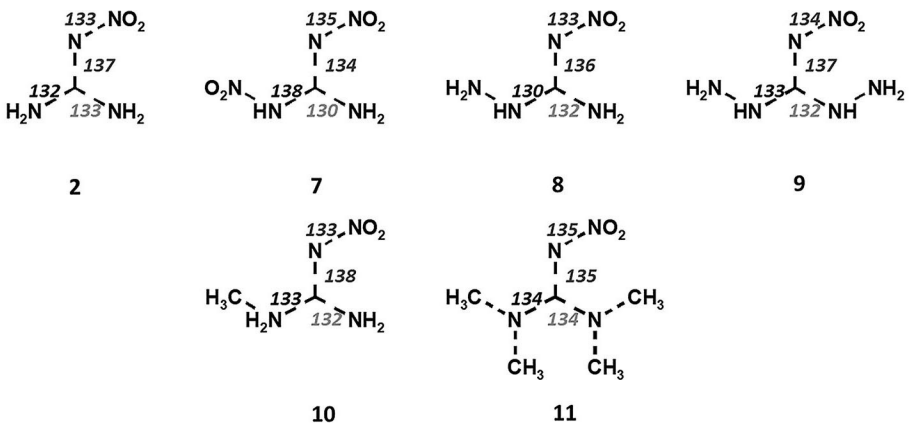

Figure 26. Bond length of some nitroguanidines in pm.

In another study *Hope & Pulham et al.* obtained 1:1 co-crystals from a D_2O-solution of [$^2D_4$]-NGu with [$^2D_3$]-2-hydroxy-3,5-dinitropyridine (DNP) (Table 12) [125]. Figure 28 shows the unit cell with four (4) formula units [$^2D_4$]-NGu:[$^2D_3$]-DNP. Figure 29 shows the arrangement of both molecules in one of the layer planes.

Table 12. [$^2D_4$]-NGu:[$^2D_3$]-DNP co-crystal properties [125].

Unit	
m_r (g mol^{-1})	296.207
V (Å^3)	1101.3966(4.1)
Z (–)	4
ρ (g cm^{-3})	1.786

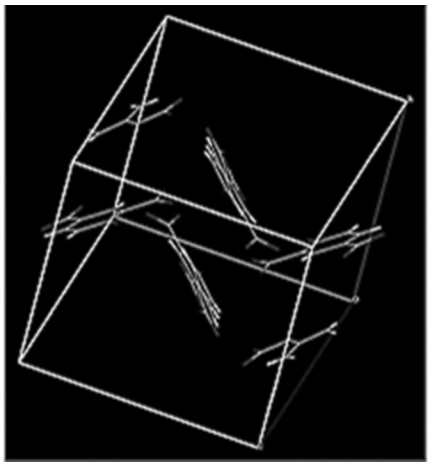

Figure 28. Unit cell of [$^2D_4$]-NGu: [$^2D_3$]-DNP co-crystal (*courtesy of K. Hope & C. Pulham*).

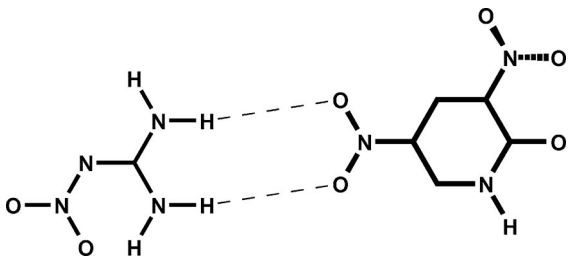

Figure 29. Lateral arrangement of [$^2D_4$]-NGu and [$^2D_3$]-DNP in co-crystal.

A high pressure/diffraction-study of the co-crystal up to $p \sim 2.8$ GPa showed a p/V-discontinuity between $p \sim 1$–1.4 GPa possibly indicating a phase transition [125]. Work is currently underway to solve the exact structure of the co-crystal and to elucidate the nature of the p/V discontinuity [126].

Jiang et al. have prepared co-crystals by vacuum freeze drying of solutions containing NGu and HMX as well as NGu and CL-20 respectively [127,128]. The identity of the co-crystals is derived mainly from interpretation of FTIR vibrations in co-crystals, raw materials and physical mixtures. Though XRD and Raman plots are reproduced these are depicted with heavy lines in thumbnail quality. In addition, both papers from *Jiang et al.* lack substantial supporting information with peak tables and highly resolved plots. Cl-20/NGu co-crystals are the subject of a Chinese patent using a different preparation method (slow evaporation of the solvent) [129]. The authors present cut-outs from the exact same IR spectra depicted in Figure 5 in Ref. [127] to manifest the identity of their co-crystals. Surprisingly the IR spectrum of their physical mixture of Cl-20/NQ in the patent is identical with the IR spectrum of the alleged co-crystal in Figure 5 of Ref [127] (sic!).

Remark: There are publications on NGu-based co-crystals by *Yong-xiang LI, Shu-sen CHEN* at Beijing Institute of Technology, and *Fu-de REN* at North University of China, Taiyuan, China. Their work assumes that NGu has the erroneous structure **B** in Figure 2 and is consequently of no use in predicting future NGu-based co-crystals, hence their work is not referred to in this review.

6 Spectroscopy

6.1 X-Ray Photoelectron Spectroscopy (XPS)

As the chemical shift related to binding energy of the N(1 s) electron covers a range of $E \sim 10$ eV XPS has been used to study the identity and simultaneously (radiation induced) the decomposition of energetic materials [130]. XPS of NGu has been studied by *Lee et al.* [131] and *Beard* [132]. Table 13 shows XPS-details and chemical shifts of NGu with both HMX and TATB as reference [133]. The intensities of the nitrogen peaks (**N**H_2, –**N**=:**N**O_2) in NGu spectra is approximately 3:1.

Table 13. XPS of NGu.

Reference	Radiation	**C** (eV)	**N**H_2; –**N**= (eV)	**N**O_2 (eV)
[131]	Al-Kα (1486.6 eV)	288.0	399.0	405.3
[132]	Mg-Kα (1253.6 eV)	–	399.9	406.3
[133] (*TATB*)	Mg-Kα (1253.6 eV)	285.0	399.0	404.6
[132] (*HMX*)	Mg-Kα (1253.6 eV)		401.4	406.9

6.2 UV-Vis Absorption Spectroscopy

The colourless solutions of NGu in aqueous media yield two distinct absorptions in the UV at $\lambda_{max} = 218$ nm (log $\varepsilon \sim 3.8$) and $\lambda_{max} = 266$ nm (log $\varepsilon \sim 4.2$) due to NH_2 and NO_2 respectively (see Figure 30) [134]. *Bisset et al.* have observed a

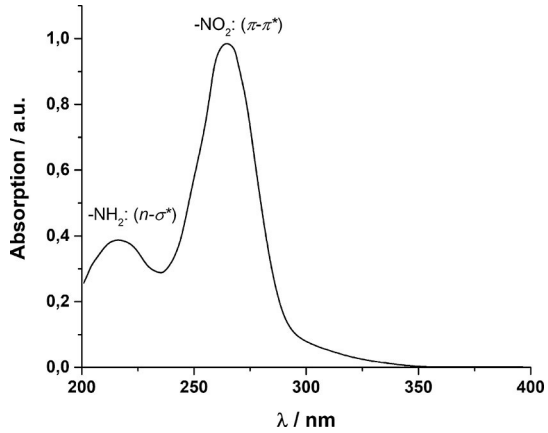

Figure 30. UV-spectrum of neutral aqueous solution of nitroguanidine (courtesy of *AlzChem Trostberg GmbH*).

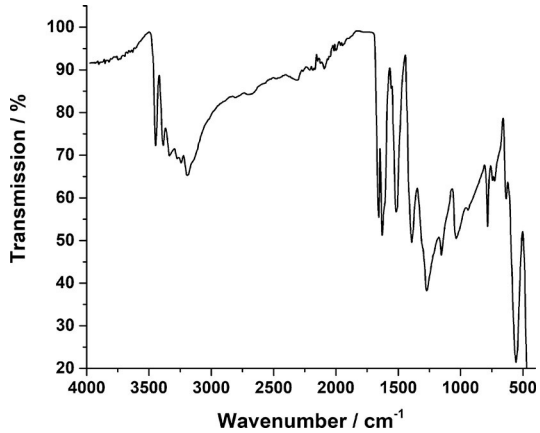

Figure 31. FTIR spectrum of NGu in ATR cell (*courtesy of AlzChem Trostberg GmbH*).

significant shift of π-π* to $\lambda_{max} = 246$ nm in strongly alkaline media with a concomitant decrease of intensity at $\lambda_{max} =$ 264 nm [135].

6.3 Optical Index of Refraction

The optical index of refraction of NGu is given in Table 14.

Table 14. Index of refraction at 598.3 nm and 25 °C.

Reference	α	β	γ
[71]	1.518	1.668	1.768
[103]	1.526	1.694	1.81

6.4 Infrared and Raman Spectroscopy

The infrared spectrum of NGu is depicted in Figure 31. Table 15 lists the peaks and gives assignments [134]. The isotopologues [$^{15}N_4$]-NGu, CAS-No: [112606–64–1], and [$^{2}D_4$]-NGu, CAS-No: [924657-59-0], have been prepared and investigated by *Morozova et al.* [136].

The FT-Raman spectrum is depicted in Figure 32, the peak list is given in Table 16.

6.5 Terahertz Spectroscopy

THz-Time Domain Spectroscopy (TDS) is a viable method for real time detection of explosives. It is based on low energy vibrational modes and in case of condensed matter on phonon modes.

Table 15. Calculated and experimental vibrational frequencies for NGu after Ref. [136].

Assignment	NGu from Figure 31 (cm^{-1})	[$^{15}N_4$]-NGu (cm^{-1})	[$^{2}D_4$]-NGu (cm^{-1})
NH(D) stretching	3445, s	3460, s	2600
	3387, s	3402, s	2565
	3332, s	3350, s	2510
	3193, s	3262	2475
NH(D) deformation	1659, s	1668, s	1619
	1632, s	1637, s	1605
NO_2 stretching	1519, s	1527	1530
	1392, s	1376	
	1308, sh		1319
	1272, vs	1287	1280
Fingerprint	1154, s	1147	1135
	1032, s	1040	1100
	941, sh	940	840
	783, s	765	785
	746, m		
	728, m	728	722
	634, m	637	590
	553, vs	570	540
	438, vs	440	430

Figure 33 depicts the THz-TDS of NGu. THz-TDS of [$^{2}D_4$]-NGu and the NGu-containing high explosive IMX-101 has been investigated in Refs. [140, 141].

6.6 Nuclear Magnetic Resonance Spectroscopy

6.6.1 ^{1}H-NMR Spectroscopy

A single resonance observed in the solid state ^{1}H-NMR spectrum of NGu provided the first proof for the nitrimine structure (**A**, Figure 2) in 1957 [142]. A single broad resonance is also observed in different solvents (Table 17).

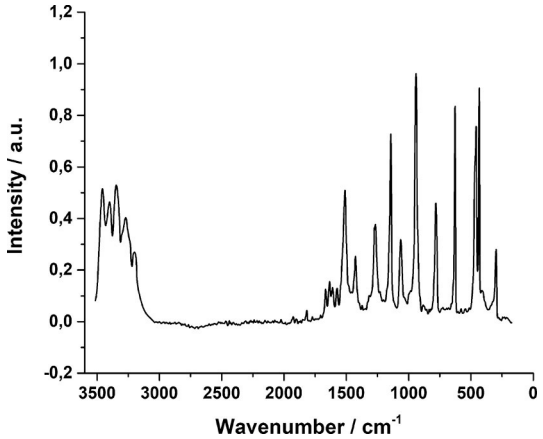

Figure 32. FT-Raman spectrum of NGu (*courtesy of AlzChem Trostberg GmbH*).

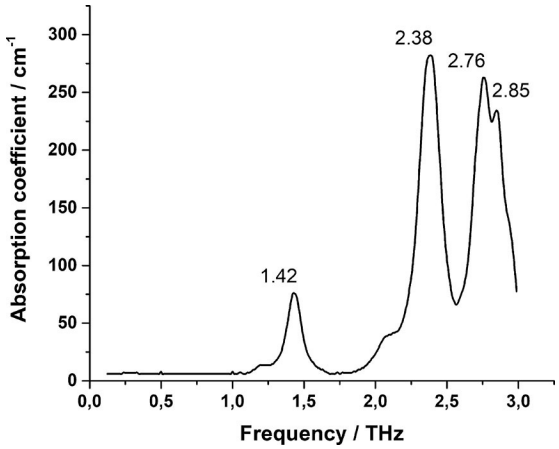

Figure 33. THz-TDS of NGu [139] with peak labels in THz.

Table 16. Raman shifts for NGu [137, 138].

Shift (cm^{-1})	Intensity
3454	s
3397	s
3348	s
3269	s
3195	m
1668	w
1634	w
1610	w
1576	w
1509	s
1424	m
1265	m
1145	vs
1064	m
943	vs
782	s
626	vs
460	vs
432	vs
298	m

Table 17. Ambient temperature ^{1}H-NMR chemical shift, δ, for amine protons (H1–H4) in NGu in different solvents.

Solvent	Frequency (MHz)	δ (ppm)	Ref.
DMSO-d_6 (25 °C)	60	7.5(2)	[143]
TFAA-d (25 °C)	60	7.8(2)	[143]
acetone-d_6 (25 °C)	600.13	7.18	[144]

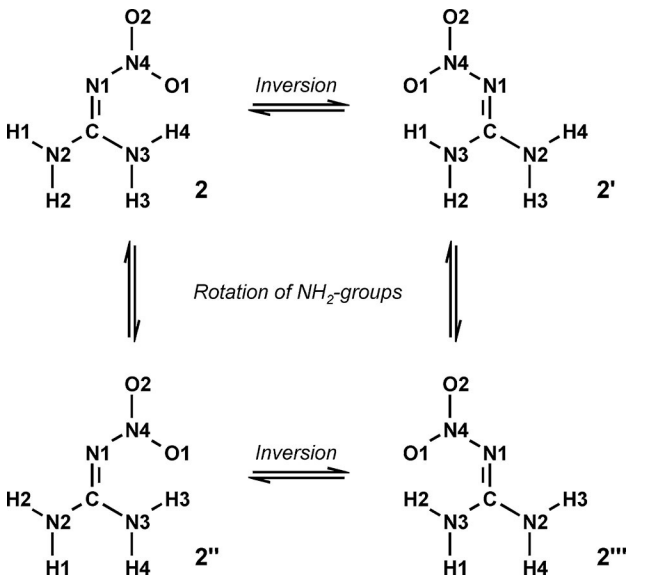

Figure 34. Exchange processes in NGu observed with NMR spectroscopy.

The chemically identical but magnetically different protons H1, H2 versus H3, H4 exchange fast enough at ambient temperature rendering structures **2** vs **2**′ and **2**′′ vs **2**′′′ indistinguishable on the NMR time scale (Figure 34). At T = 48 °C in acetone-d_6 the resonance signal is a sharp peak at δ = 7.10 ppm, whereas at T = 15 °C the signal broadens significantly. At T = 2 °C the signal assumes the typical trapezoidal shape indicative of a coalescence point. Further cooling to T = −10 °C results in two clearly separated but still broadened signals that in spite of increased solvent viscosity become very sharp again at T = −44 °C), δ = 7.94 ppm and 7.12 ppm respectively.

Line-shape analysis of the dynamic spectra yields a free activation enthalpy for the isomerisation process, $\Delta G^{\neq}$ = 26 kJ mol^{-1} [144]. The signal at lower field (δ = 7.93 ppm) is assigned to the protons de-shielded by interaction with O1 (intramolecular hydrogen bond). A lower signal intensity for latter than for the other protons could be indicative of yet another exchange process (2, 2′ versus 2′′,2′′′). A similar exchange process has been observed to occur with FOX-7 (**3**)

Table 18. ^{15}N-NMR Chemical shift [$^{15}N_4$]-nitroguanidine.

Ref.	Frequency (MHz)	Details	N1 (ppm)	N2 (ppm)	N3 (ppm)	N4 (ppm)
[139]	20.727	CP/MAS	−144 ϕ: 103 Hz	−294 ϕ: 237 Hz	−294 ϕ: 237 Hz	−11 ϕ: 65 Hz
[139]	20.727	DMSO-d_6	−135 $^1J(^{15}N^{15}N)$: 15.4 Hz 1 $J(^{15}N^{13}C)$: 19 Hz	−293 $^1J(^{15}N^1H)$: 91.8 Hz	−293 $^1J(^{15}N^1H)$: 91.8 Hz	−6 $^1J(^{15}N^{15}N)$: 15.4 Hz
[140]	40.55	DMSO-d_6	−142.5	299.6	299.6	−12.7

*relative to $CH_3{}^{15}NO_2$, ϕ = full width at half maximum (Hz) for MAS peaks.

[145]. As of yet the exact mechanism of the exchange process in NGu (*N1* inversion versus C–N1-rotation) is unclear though concepts exist to describe related materials [146–148].

6.6.2 ^{15}N-NMR Spectroscopy

Despite the low natural abundance (0.365 wt.-%), low responsivity (15N : 0.001 vs ^{1}H : 1.000) and the long relaxation times T_1, the chemical shift of ^{15}N stretches over nearly 900 ppm (not including transition metal complexes). This allows for very characteristic chemical assignments [149].

The ambient temperature ^{15}N-NMR/MAS spectrum of crystalline [$^{15}N_4$]−nitroguanidine yields three peaks (Table 18) [150] in accordance with the nitrimine structure (A, Figure 2) and a rapid exchange process as indicated in Figure 34 leading to magnetic equivalence of N2 and N3. The exchange process itself and the $^1J(^{15}N^1H)$1H yields a significant broadening of the signal with a ϕ of 237 Hz.

The ^{15}N-NMR spectra in DMSO-d_6 are in full accord and show $^1J(^{15}N^{15}N)$ coupling between N1 and N4. In addition, both N2 and N3 show a well resolved triplet structure due to $^1J(^{15}N^1H)$: 91.8 Hz. The observed small chemical shift for N4 is typical for NO_2 groups. Likewise, is the signal for the NH_2–nitrogen atoms (N2, N3). The chemical shift for typical imino–nitrogen atoms (e.g. in guanidine and many of its acyclic and cyclic derivatives including cyanoguanidine) ranges between $\delta = -170$–300 ppm [151,152]. However, in nitroguanidine the resonance for the imino–nitrogen is observed at significantly lower field ($\delta = -135$ ppm). This deshielding can be explained with the ionic resonance structures depicted in Figure 25. The methylnitramide anion (**12**$^-$) compares well with those resonance structures of NGu (Figure 35). Whereas the amine nitrogen in methylnitramide, $CH_3NH–NO_2$ (**12**), has its resonance at $\delta = -224.3$ ppm, the imine nitrogen in its anion, **12**−, appears at $\delta = -121.7$ ppm which is close to the N1 resonance (δ: −142.5 ppm) [151].

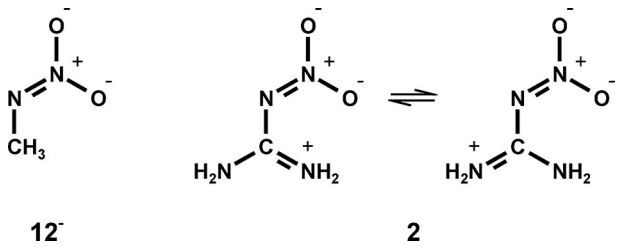

Figure 35. Structural and electronic similarity between methylnitramide anion, **12**$^-$ and NGu.

6.6.3 ^{13}C-NMR Spectroscopy

The ^{13}C-NMR spectrum in DMSO-d_6 shows one signal, $\delta =$ 160 ppm with triplet structure due to $^1J(^{15}N^{13}C)$: 19 Hz coupling with both amine nitrogen atoms (Table 19) [150]. The geminal coupling with the imine nitrogen, N1, as well as vicinal coupling with N4 are not resolved which is not unusual [153].

Table 19. ^{13}C-NMR of NGu [150].

Solvent	Frequency (MHz)	δ (ppm)
DMSO-d_6 (25 °C)	50.311	160; $^1J(^{13}C^{15}N)$: 19 Hz

6.6.4 ^{14}N-NQR Spectroscopy

^{14}N-nuclear quadrupolar resonance is a method investigated both for detection of high explosives [154] as well as material investigation [155]. Unlike nitramines which show clear distinction between different nitrogen atoms, NGu yields one peak only $\delta = 327$ ppm [156].

6.7 Mass Spectrometry

Figure 36 depicts the mass spectrum of NGu, Figure 37 indicates the underlying decomposition process.

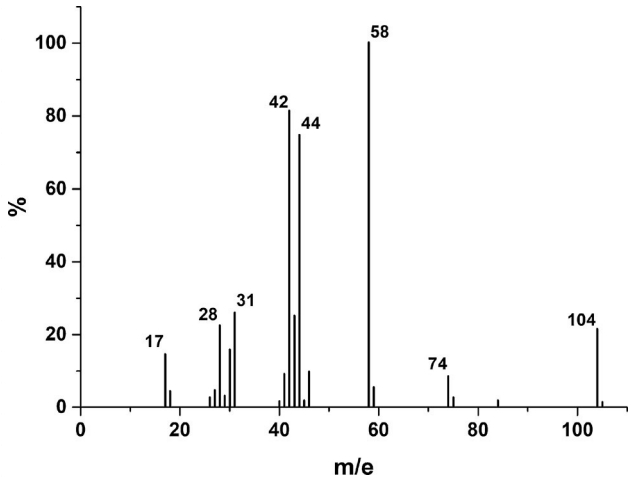

Figure 36. Mass spectrum of NGu after [157].

Other MS spectrometric data can be found in Ref. [158].

7 Safety and Sensitiveness of NGu

NGu is the proverbial insensitive high explosive. Its low sensitiveness derives from the molecular structure (intramolecular hydrogen bonds, iminium nitronate structure) and crystal structure (intermolecular hydrogen bonds) allowing for easy dissipation of energy (Figure 35). The high nitrogen content further effects poor thermal ignition and combustion behaviour [159]. Consequently, formulations containing NGu and avoiding sensitive material often pass stringent IHE or UN Test Series 7 tests and can be classified accordingly as EIS (*formerly designated EIDS*) [160]. Within the context of this review only the response of pure NGu and NGu wetted with water will be considered. The vulnerability of NGu-based formulations will be dealt with an upcoming paper. In the following NGu is compared to related FOX-7, TATB and FOX-12.

7.1 Hazard Classification of NGu

Dry NGu is classified as HD 1.1 D. Nitroguanidine wetted homogeneously with at least 20 wt.-% water is a solid "desensitized explosive" and is classified as HD 4.1 [161]. Its response in comparison to dry material with regards to selected test from ref. [162] is displayed in Table 20.

7.2 Friction and Impact Sensitivity

NGu is not friction sensitive in the BAM test (UN Test Series 3 (b)(i).

NGu is not impact sensitive in the BAM test (UN Test Series 3(a)(ii) (> 50 J), with the 30 kg Fallhammer-test (UN Test series 3(a)(iv) and is not impact sensitive in the ERL-LASL impact test (> 320 cm with both type 12 and 12B tool) [163]. This reaction puts NGu on a par with TATB, however it is less sensitive than both FOX-7 and FOX-12.

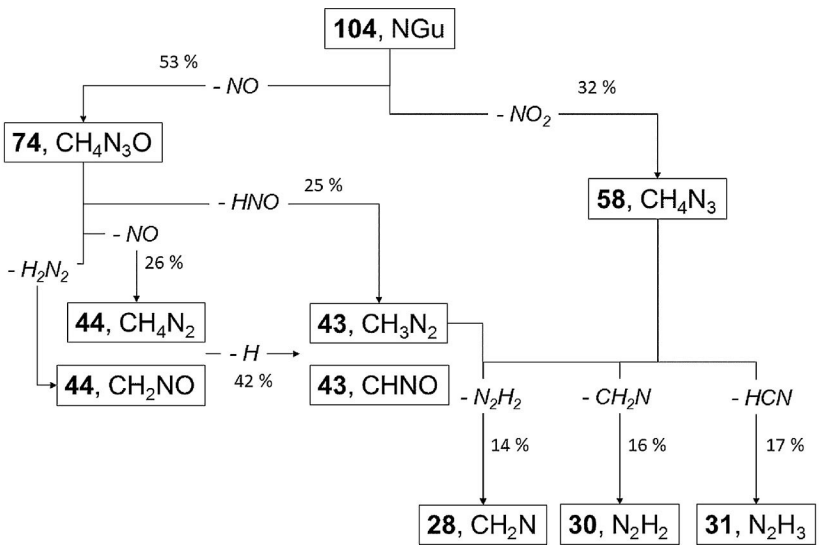

Figure 37. Decomposition pathways in the mass spectrum of NGu [157].

Table 20. UN Test results on dry and wetted NGu (> 20 wt.-% water) after Ref. [161].

UN-Test [162]	Dry NGu	NGu wetted with > 20 wt.-% Water
1(a)(i) BAM steel tube test	Not tested	"−" (no propagation)
1(a)(iii) Gap Test: 0 mm	"+"	Not tested
2(a)(iii) Gap Test: 57.2 mm	"−"	Not tested
2(a) (iii) Gap Test: 50.8 mm	"+"	Not tested
5(a) Cap Sensitivity PETN (0.6 g)	"+"	"−"
6(c) Bonfire test	Not tested	"−"

7.3 Thermal Response

At the highest temperature in the Henkin Test, 367 °C NGu does not react [164], whereas TATB reacts after ~111 s [165]. In the ODTX test NGu yields an explosion at T = 313 °C/12 s which is lower than TATB [166] but higher than FOX-7 [167]. The good-natured behaviour of NGu upon fast confined heating (FCO) in the Koenen test (UN Test Series 1(b)) is exemplary for an insensitive energetic material with no explosion occurring (Type C; negative reaction) even at the narrowest orifice plate (1 mm) conceived for this test [168]. Both FOX-7 [167] and FOX-12 [169] do react more violently and yield at least three fragments at even larger orifice diameters (Type F; positive reaction) see Table 20. As the other materials NGu is not sensitive to ESD either.

7.4 Shock Sensitivity

NGu is extremely insensitive towards shock as is evident from results of the NOL-LSGT [170]. The P_{50} pressure is 30–50% higher than for insensitive High explosives, FOX-7, TATB and FOX-12 (Table 21).

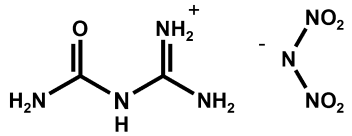

6

Figure 38. Structure of *N*-guanylurea dinitramide, (**6**), FOX-12.

8 Summary

Nitroguanidine is an insensitive high nitrogen compound fulfilling multiple roles as energetic filler in triple base and insensitive, low erosion gun propellants, rocket propellants, gas generators, pyrotechnics and insensitive high explosives. It is produced in a straightforward manner in good overall yield in a sustainable process from basic raw materials: coke, lime stone, and dinitrogen. Only one crystallographic form of NGu is known at ambient temperature and pressure though crystallisation from various media yields a broad range of particle morphologies ranging from long needles over jolted prisms to nice spherulitic grains with high bulk densities. In the solid state nitroguanidine maintains a number of hydrogen bonds to its next neighbours giving rise to poor solubility in protic polar solvents but good solubility in aprotic polar solvents. Crystallographic investigations and spectroscopic data indicate that NGu is best described with ionic canonical resonance structures of the iminium nitronate type depicted in Figure 35. When NGu is compared with FOX-12 and its structural relatives FOX-7 and TATB it turns out that NGu is the least sensitive towards mechanical and thermal stimuli. Though NGu is classified as an explosive in the dry state when wetted with > 20 wt.-% water it becomes a desensitized explosive and is classified under Hazard Division 4.1 which enables comparingly facile logistics.

Table 21. Sensitiveness of NGu, FOX-7, TATB and FOX-12.

	NGu (**2**)	FOX-7 (**3**)	TATB (**4**)	FOX-12 (**6**)
Friction BAM (N)	> 355	160–240	> 355	> 352
Impact BAM (J)	> 50	15–30	> 50	31
Impact 30 kg (m)	> 4			
T_i (°C)	does not ignite	–	–	200–225
ODTX (°C s^{-1})	313/12	260/15*)	370/70	n.a.
Koenen (mm/Type)	< 1/C[a)]	6/F[b)]	?	2/F
NOL-LSGT-P_{50} (GPa)	9.07(1.64 g cm^{-3})	4–6.5	6.58 (1.82 g cm^{-3})	6–7 (at 1.66 g cm^{-3})

*FOX-7/Viton® A (95/5); #) shock sensitivity decreases with increasing particle size: (37→358 μm); a) C: Bottom of tube split; b) F: Tube fragmented into three or more large pieces which in some cases may be connected with each other by a narrow strip. *Abbreviations:* NOL-LSGT-P_{50} = 50%-Initiation Pressure in the Naval Ordnance Laboratory, Large Scale Gap Test (GPa); T_i = Ignition temperature (°C); ODTX = Temperature and time to explosion (°C s^{-1}); Koenen = Limiting orifice diameter and type of reaction in Koenen test.

9 Outlook

An upcoming paper reviews the detonative performance and vulnerability (thermal, shock) of NGu based high explosive formulations as well as the occupational and environmental footprint of NGu.

10 Remarks

Crystallographic depictions of NGu displayed in this article have been prepared with CCDC dataset # 1223553, based on Ref. [6] using *Mercury 3.10.2 crystallographic software*, Copyright © **2017** Cambridge Crystallographic Data Centre, UK.

Abbreviations

a, b, c	Lattice constants (pm)
ARC	Adiabatic self-heating onset temperature (°C)
A_S	Specific Surface Area ($m^2 g^{-1}$)
ATR	Attenuated Total Reflection
BAF	British Aqueous Fusion Process
BMR	Boatright Mackay Robert Process
c	Concentration ($mol^{-1} l^{-1}$)
CAS	Chemical Abstracts Service
c_L	Velocity of sound (longitudinal) ($m s^{-1}$)
c_p	Specific heat ($J g^{-1} K^{-1}$)
CP	Circular polarized
CONUS	Continental United States
d	Diffraction spacing (Å)
DCD	Dicyandiamide, $C_2H_4N_4$
d_{hkl}	Interplanar distance (pm)
DMF	Dimethylformamide, C_3H_7NO
DMSO	Dimethylsulphoxide, C_2H_6SO
DNAN	2,4-Dinitroanisole, $C_7H_6N_2O_5$
DNP	2-Hydroxy-3,5-dinitropyridine, $C_5H_3N_3O_5$
E_{att}	Attraction force ($kJ mol^{-1}$)
EI(D)S	Extremely Insensitive (Detonating) Substance (formerly *EIDS* now *EIS*)
EG	Ethylene glycol, $C_2H_6O_2$
FOX-7	1,1-Diamino-2,2-dinitroethylene, $C_2H_4N_4O_4$
FOX-12	*N*-Guanylurea dinitramide, $C_2H_7N_7O_5$
FSSS	Fisher Sub Siever Size (μm)
GP	Gun propellants
Gu	Guanidine, CH_5N_3
GuH^+	Guanidinium, $CH_6N_3^+$
GuN	Guanidinium nitrate, $CH_6N_4O_3$
H_0	Hammett acidity function
HBD	High Bulk Density
HE	High Explosives
HMX	Octogen, $C_4H_8N_8O_8$
HNP	2-Hydroxy-5-nitropyridine, $C_5H_4N_2O_3$
IUPAC	International Union for Pure and Applied Chemistry
$^nJ(^xA^yB)$	Spin-Coupling of two nuclei (^{x}A)and (^{y}B) over *n* bonds (Hz)
LBD	Low Bulk Density
LLM-116	4-Amino-3,5-dinitro-1*H*-pyrazole, $C_3H_2N_5O_4$
MAS	Magic Angle Spinning
Mp	Melting point (°C)
m_r	Molecular mass ($g mol^{-1}$)
NGu	Nitroguanidine, $CH_4N_4O_2$
$NGuH^+$	Nitroguanidinium, $CH_5N_4O_2^+$
NMP	*N*-Methylpyrrolidone, C_5H_9NO
NMR	Nuclear Magnetic Resonance
NOL-LSGT	Naval Ordnance Laboratory, Large Scale Gap Test
NQR	Nuclear Quadrupolar Resonance
ODTX	One-Dimensional-Time-to-Explosion
p	Pressure (GPa)
P_{50}	50 % Initiation Pressure (GPa)
P_{CJ}	Detonation (Chapman Jouguet) Pressure (GPa)
pK_b	Base constant ($-\log_{10} K_b$)
R	Relative growth velocity
RP	Rocket Propellants
S	Solubility ($g kg^{-1}$)
SFAAP	Sunflower Army Ammunition Plant
SHBD	Spherical High Bulk Density
TATB	1,3,5-Triamino-2,4,6-trinitrobenzene, $C_6H_6N_6O_6$
TDS	Time Domain Spectroscopy
T_{dec}	Decomposition temperature (°C)
TFAA	Trifluoroacetic Acid Anhydride, $C_4F_6O_3$
T_i	Ignition temperature (°C)
UF	Ultrafine (submicron)
UV	Ultraviolet range ($\lambda = 200$–400 nm)
V	Volume of unit cell ($Å^3$)
V_D	Detonation Velocity ($m s^{-1}$)
XPS	X-Ray Photoelectron Spectroscopy
Z	Number of formula units in unit cell (–)
δ	Chemical shift in NMR (ppm)
$\Delta_{ex}H$	Enthalpy of explosion ($kJ mol^{-1}$)
$\Delta_f H$	Enthalpy of formation ($kJ mol^{-1}$)
$\Delta G\neq$	Free Enthalpy of Activation ($kJ mol^{-1}$)
ε	Extinction coefficient ($\log cm^2 mol^{-1}$)
ϕ	full width at half maximum (Hz)
κ	Thermal conductivity ($W m^{-1} K^{-1}$)
Ω	Oxygen balance (wt.-%)
N	Nitrogen Content (wt.-%)
ρ	Density ($g cm^{-3}$)
$\sqrt{2E_G}$	Gurney Velocity ($m s^{-1}$)
2θ	Diffraction reflex (°)

Acknowledgements

The author thanks *Prof. Dr. Colin Pulham* & *Dr. Karl S. Hope* (Edinburgh University, UK), for helpful discussion and kind permission to reproduce picture of unit cell of NGu–DNP co-crystal (Figure 28). The author thanks *Dr. Rainer Schirra*, (DynITEC, Troisdorf, Germany) for helpful discussions and kind provision of details on NGu synthesis (ref. [54, 55]. The author thanks *Prof. Dr. Ing. Andrzej Maranda,* (IPO, Warzaw, Poland) for kind permission to reproduce pictures of

recrystallised NGu (Figures 18 and 19). The author gratefully acknowledges *AlzChem Trostberg GmbH*, Trostberg, Germany for funding this work and *Dr. Frank Fleischer*, (*AlzChem Trostberg GmbH*) for helpful discussions and provision of process and analytical data on NGu. The author thanks the referees for pointing out errors and inconsistencies and for their valuable recommendations to improve the manuscript.

References

[1] E.-C. Koch, Insensitive High Explosives II: 3,3-Diamino-4,4′-azoxyfurazan (DAAF), *Propellants Explos. Pyrotech.* **2016**, *41*, 526–538.
[2] E.-C. Koch, Nitroguanidine (NQ) – An Underestimated Insensitive Energetic Material for High Explosives and Propellants, *49th International Annual Conference of ICT*, 26–29 June, **2018**, Karlsruhe, Germany, V-3.
[3] L. Jousselin, Sur la nitrosoguanidine, *Compt. Rend.* **1877**, *85* 548–550.
[4] G. Pellizzari, Nitroguanidina, *Gazz. Chim.* **1891**, *21*, 405–409.
[5] J. Thiele, Ueber Nitro- und Amidoguanidin, *Ann. Chem.* **1892**, *270*, 1–63
[6] C. S. Choi, Refinement of 2-Nitroguanidine by Neutron Powder Diffraction, *Acta Cryst.* **1981**, *B37*, 1955–1957.
[7] E.-C. Koch, *Sprengstoffe Treibmittel Pyrotechnika*, Lutradyn, Kaiserslautern, **2018**, pp. a) 146; b) 342–343; c) 228.
[8] J. Bellamy, FOX-7(1,1-Diamino-2,2-dinitroethene), in T. M. Klapötke (ed.) *High Energy Density Materials*, Struct. Bond. **2007**, *125*, 1–33.
[9] B. Dobratz, The Insensitive High Explosive Triaminotrinitrobenzene (TATB): Development and Characterization – 1888 to 1994, *LA-13014H*, Los Alamos National Laboratory, **1994**, 152 pp.
[10] R. D. Schmidt, G. S. Lee, P. F. Pagoria, A. R. Mitchell, R. Gilardi, Synthesis and Properties of a New Explosive, 4-Amino-3,5-dinitro-1*H*-pyrazole, *UCRL-ID-148510*, Lawrence Livermore National Laboratory, USA, **2001**, 29 pp.
[11] B. T. Fedoroff, Dictionary of Explosives, Ammunition and Weapons (German Section), Picatinny Arsenal, **1958**, pp. Ger-121–122.
[12] B. T. Fedoroff, *Encyclopedia of Explosives and Related Items*, *Volume 6*, Picatinny Arsenal, **1974**, pp. G-154–159.
[13] T. M. Klapötke, *Energetic Materials Encyclopedia*, De Gruyter, Berlin, **2018**, a) pp. 210–212; b) 305–308.
[14] B. M. Dobratz, P. C. Crawford, *LLNL Explosives Handbook Properties of Chemical Explosives and Explosive Simulants*, Lawrence Livermore National Laboratory, University of California, Livermore, CA, USA, **1985**, pp. 19–101-19–102.
[15] https://www.alzchem.com/en/nitroguanidine accessed on July 7, **2018**.
[16] R. Ritter, F. Walter, Carbid, Kalkstickstoff und Siliciumcarbid in K. Winnacker (Ed.) *Chemische Technologie – Anorganische Technologie II*, Carl Hanser Verlag, München, **1950**, pp. 247–284.
[17] NN., Verfahren zur Herstellung von Diamid- (Hydrazin-) hydrat bezw. dessen Salzen, DE-Patent 59241, **1891**, BASF, Deutschland.
[18] H. Gockel, Verfahren zur Darstellung von Guanidinsalzen aus Rhodanammonium, DE-Patent 611945, **1935**, Gockel, Deutschland.
[19] H. Gockel, Über die Gewinnung von Guanidinnitrat aus Rhodanammonium, *Angew. Chem.* **1935**, *48*,430.
[20] C. Schöpf, H. Klapproth, Über eine Explosion bei der Darstellung von Guanidinnitrat aus Rhodanammonium, *Angew. Chem.* **1936**, *49*, 23.
[21] H. McLeod, *Canada's Chemical Industries*, Dominion Bureau of Statistics, Ottawa Canada, **1947**, pp. 14, 59, 63; accessed on August 13 2018 at http://publications.gc.ca/collections/collection 2016/statcan/CS46-D-50-1947-eng.pdf
[22] W. H. Hill, *Preparation of Guanidine Nitrate*, US Patent 2468067, **1949**, Koppers Company Inc., USA.
[23] T. L. Davis, *Procédé de préparation du nitrate de guanidine*, FR-Patent 539125, USA, Davis, **1922**.
[24] T. L. Davis, *The Chemistry of Powder and Explosives*, John Wiley, New York, **1941**, p. 375.
[25] W. Moschel, G. Broja, *Verfahren zur kontinuierlichen Herstellung von Guanidinsalzen*, DE-Patent 908612, Deutschland, Bayer AG, **1954**.
[26] J. H. Paden, K. C. Martin, R. C. Swain, Guanidine Nitrate from Dicyandiamide and Ammonium Nitrate by Pressure Reaction, *Ind. Eng. Chem.* **1947**, *39*, 952–958.
[27] F. Hofwimmer, *Verfahren zur Herstellung von Guanidinsalzen*, DE-Patent 332681, **1921**, Hofwimmer, Germany.
[28] G. F. Wright, *Preparation of Guanidine Nitrate*, US-Patent 2431301, Canada, The Honorary Advisory Council for Scientific and Industrial Research of Canada, Canada **1947**.
[29] D. Sh. Rozina, R. L. Globus, R. P. Lastovskii, P. A. Voronin, A. S. Tseitlenok, T. I. Generalova, P. D. Yakukhnyi, A. F Nagornyi, B. S. Rubinson, *Guanidine nitrate*, SU-Patent 106838, **1957**, NN., Soviet Union.
[30] J. W. Leach, Detonation of Guanidine Nitrate and Nitroguanidine Manufacture via U/AN and BAF Process, *Technical Report ARLCD-TR-78062*, US Army Armament Research and Development Command, August **1979**, 50 pp.
[31] L. G. Boatright, J. S. Mackay, *Preparation of Guanidine Salts and Substituted Guanidine Salts*, US-Patent 2783276, **1957**, American Cyanamide Company, USA.
[32] E. Roberts, T. Martin, *Manufacture of Guanidine Nitrate*, US-Patent 3043878, **1962**, Her Majesty's Government of the United Kingdom and Northern Ireland, Great Britain.
[33] J. S. Mackay, *Preparation of Guanidine Compounds*, US-Patent 2949484, **1960**, Pittsburgh Coke & Chemical Company. USA.
[34] N. W. Steele, Process Engineering Design for Manufacture of Guanidine Nitrate, Hercules Inc. 1973, *ADA-772074*, December **1973**, USA.
[35] T. H. Chen, W. F. Ark, C. Ribaudo, W. J. Fisco, F. X. Murphy, H. Kramer, T. C. Castorina, Modern Methods of Analysis for Control of Continuous Nitroguanidine Process, *ARLCD-SP-81001*, US Army Armament Research and Development Command, Dover NJ, USA, May **1981**, 88 pp.
[36] A. Golius, L. Gorb, A. M. Scott, F. C. Hill, D. Felt, S. Larson, J. Ballard, J. Leszcynski, Computational Study of nitroguanidine (NQ) tautomeric properties in aqueous solutions, *Struct. Chem.* **2015**, *26*, 1273–1280.
[37] M. D. Pace, J. L. Flippen-Anderson, Crystal structures and EPR spectra of nitroguanidine chloride and nitroguanidine nitrate, *J. Energ. Mater.* **1984**, *2*, 43–60.
[38] R. J. J. Simkins, G. Williams, The Nitration of Guanidine in Sulphuric Acid. Part I. The Reversible Conversion of Guanidine Nitrate into Nitroguanidine, *J. Chem. Soc.* **1952**, 3086–3094.
[39] H.-J. Riedl, W. Sauermilch, *Verfahren zur Herstellung von Nitroguanidin*, DE-Patent 1143194, **1963**, Wasag Chemie AG, Deutschland.
[40] V. Y. Rosolovskii, K. V. Titova, Nitroguanidinium Perchlorate, *Russ. J. Inorg. Chem.* **1966**, *11*, 1515–1516.

[41] G. Steinhauser, M.-J. Crawford, C. Darwich, T. M. Klapötke, C. Miró Sabaté, J. M. Welch, The energetic double salt nitroguanidinium nitrate–guanidinium nitrate (1/1), *Acta Cryst.* **2007**, *E63*, o3100–o3101.

[42] W. McBride, R. A. Henry, J. Cohen, S. Skolnik, Solubility of Nitroguanidine in Water, *J. Am. Chem. Soc.* **1951**, *73*, 485–486.

[43] J. B. Morris, Extraction of Nitroguanidine (NQ) from Triple-Base Gun Propellant, *ARL-TR-2669*, Army Research Laboratory, Aberdeen, MD, USA, **2002**, 18 pp.

[44] Y. Y. Orlova, *The Chemistry and Technology of High Explosives*, *Part II*, English Translation, Foreign Technology Division, Technical Documents Liaison Office, Wright-Patterson Air Force Base, Dayton, OH, USA, **1961**, pp. 557–564.

[45] W. Schemuth, Verfahren zur Herstellung von schwefelsäurefreiem Nitroguanidin mit großer spezifischer Oberfläche, DE-Patent 1010888, **1957**, Schemuth, Deutschland.

[46] G. Williams, R. J. J. Simkins, The Nitration of Guanidine in Sulphuric Acid. Part II. Kinetics of N-Nitration of the Guanidinium Ion and Denitration of Nitroguanidine, *J. Chem. Soc.* **1953**, 1386–1392.

[47] J. C. Oxley, J. L. Smith, J. S. Moran, J. N. Canino, J. Almog, Aromatic nitration using nitroguanidine and EGDN, *Tetrahedron Lett.* **2008**, *49*, 4449–4451.

[48] Y. Bayat, F. Hajighasemali, Synthesis of CL-20 by a Greener Method Using Nitroguanidine/HNO_3, *Propellants Explos. Pyrotech.* **2016**, *41*, 20–23.

[49] T. G. Bonner, J. C. Lockhart, The Denitration of Nitroguanidines in Strong Acids. Part I. The Correlation of Rate Constants with the Acidity Function, H_0, and Activities of Solvent Entities, *J. Chem. Soc.*, **1958**, 3852–3858.

[50] T. G. Bonner, J. C. Lockhart, The Denitration of Nitroguanidines in Strong Acids. Part II. Absorption Spectra and pKa Values of Certain Nitroguanidines, *J. Chem. Soc.*, **1958**, 3858–3861.

[51] K. Schofield, *Aromatic Nitration*, Cambridge University Press, Cambridge, **1980**, p. 31.

[52] M. Thoma, *Verfahren zur Herstellung von Nitroguandin aus Guanidinnitrat*, DE-Patent 1234204, **1967**, Chemisches Werk Lowi, Deutschland.

[53] T.-K. Liu, Y. N. Shyr, C.-Y. Ho, Kinetics of Dehydration of Guanidine Nitrate in H_2SO_4/HNO_3/H_2O Ternary Mixtures, *Propellants Explos. Pyrotech.* **1990**, *15*, 143–148.

[54] R. Schirra, On a New Synthesis of Nitroguanidine (NQ), *DEA-Meeting*, Troisdorf, September **1999**, Germany.

[55] W. Pabst, A. Busch, R. Schirra, *Verfahren zur Herstellung von Nitroguanidin*, DE-10065938A1, **2001**, Dynamit Nobel GmbH, Deutschland.

[56] A. A. Astrat'ev, D. V. Dashko, A. I. Stepanov, Study of the Routes for Producing Nitroguanidine (NQ) in Aqueous Nitric Acid Solutions. Development of the efficient method for synthesis, *9th Seminar New Trends in Research of Energetic Materials*, Pardubice, Czech republic, 19–21 April **2006**, pp. 377–392.

[57] C. Kang, Z. Luo, Y. Yang, M. Li, S. Chen, Reaction kinetics of nitroguanidine prepared by nitrate method, *Chemical Engineering (China)*, **2015**, *43*, 56–59.

[58] M.-D. Marqueyrol, P. Loriette, *Perfectionnnement à la préparation de la nitroguanidine à partir de la dicyandiamide*, FR503741, **1920**, Marqueyrol & Loriette, France.

[59] J. Mayer, *Verfahren zur Herstellung von Nitroguanidin*, DE-Patent 958833, Deutschland, Fa. Josef Meissner, **1957**.

[60] J. R. C. Duke F. J. Llewellyn, The crystal structure of ammonium trinitrate, $NH_4NO_3 \cdot 2HNO_3$, *Acta Cryst.* **1950**, *3*, 305–311.

[61] B. Unterhalt, N–Nitro–imine, in D. Klamann, H. Hagemann (Eds.), Methoden der Organischen Chemie (Houben-Weyl), E 14 b: Organische Stickstoff-Verbindungen mit einer C,N-Doppelbindung, Thieme, Stuttgart, **1990**, pp. 769–779.

[62] G. W. Watt, R. C. Makosky, Synthesis of Guanidine and Nitroguanidine, *Ind. Eng. Chem.* **1954**, *46*, 2599–2604.

[63] G. Gattow, T. Kuhlmann, *N*-Hydroxyguanidin, *Z. Anorg. Allg. Chem.* **1982**, *494*, 134–138.

[64] G. J. Southan, A. Srinivasan, C. George, H. M. Fales, L. K. Keefer, *N*-Nitrosated *N*-hydroxyguanidines are nitric oxide-releasing diazeniumdiolates, *Chem. Commun.* **1998**, 1191–1192.

[65] G. J. Southan, A. Srinivasan, Nitrogen Oxides and Hydroxyguanidines: Formation of Donors of Nitric and Nitrous Oxides and Possible Relevance to Nitrous Oxide Formation by Nitric Oxide Synthase, *Nitric Oxide* **1998**, *2*, 270–286.

[66] E. Ripper, G. Krien, Über α- und β-Nitroguanidin, *Explosivstoffe*, **1969**, *17*, 145–151.

[67] L. Song, L. Chen, D. Cao, J. Wang, Solvent selection for explaining the morphology of nitroguanidine crystals by molecular dynamics simulation, *J. Cryst. Growth* **2018**, *483*, 308–317.

[68] Y. Ma, A. Zhang, C. Zhang, D. Jiang, Y. Zhu, C. Zhang, Crystal packing of Low Sensitivity and High-Energy Explosives, *Cryst. Growth Des.* **2014**, *14*, 4703–4713.

[69] K. G. Shipp, T. N. Hall, M. E. Hill, Heat Resistant Explosive V. 1, 3-Diamino-2, 4, 6-Trinitrobenzene, DATB, by Ammonolysis of Methoxytrinitrobenzene Compounds, Naval Ordnance Laboratory White Oak, MD, 15. Dec **1958**, 18 pp.

[70] D. Zheng, X. Guo, H. Lin, Y. Ou, B. Dong, G. Wang, Preparation and Performance research of ultra-fine nitroguanidine, *J. Solid Rocket Tech.* **2015**, *38*, 847–852.

[71] J. Doll, E. Grison, Étude cristallographique de la nitroguanidine, *C. R. Hebd. Seances Acad. Sci.* **1948**, *226*, 679–680.

[72] M. J. Tranchant, Cristallisation de la Nitroguanidine en très fins cristaux, *Mém. Poudres* **1948**, *30*, 175–187.

[73] W. Schnurr, *On the Manufacture of Nitroguanidine* in O. W. Stickland, J. H. Ross, L. Nutting, W. J. Powell, C. D. Pratt (Eds.), General Summary of Explosive Plants DAG Krümmel, Dünneberg, Christianstadt, *CIOS Target No 2/69*, *2/70*, *2/79b*, *Explosives Propellants*, London, HMSO, **1945**.

[74] L. Reinhardt, G. Drube, *Verfahren zur Änderung der Kristalltracht von Nitroguanidin*, DE-Patent 1048528, **1959**, Wasag-Chemie AG, Deutschland.

[75] H. Brachert, *Verfahren zur Herstellung von kompaktem Nitroguanidin*, DE-Patent 2701994C2, **1986**, Dynamit Nobel AG, Deutschland.

[76] S. L. Collignon, K. L. Wagaman, *Continuous Process for Crystallizing Nitroguanidine*, US H1510, **1995**, The United States of America as represented by the Secretary of the Navy, USA.

[77] K. L. Wagaman, C. F. Clark, W. S. Jones, S. L. Collignon, M. C. Wilmot, *Method for Producing High Bulk Density Density Spheroidal Nitroguanidine*, US H1778, **1999**, The United States of America as represented by the Secretary of the Navy, USA.

[78] R. Mudryy, R. Damavarapu, V. Stepanov, R. Halder, Crystallization of High Bulk Density Nitroguanidine, *Technical Report ARMET-TR-10045*, June **2011**, Picatinny Arsenal, NJ, USA.

[79] Z. Luo, Y. Cui, W. Dong, Q. Xu, G. Zou, C. Kang, B. Hou, S. Chen, J. Gong, Morphological diversity of nitroguanidine crystals with enhanced mechanical performance and thermodynamic stability. *J. Cryst. Growth* **2017**, *480*, 132–140.

[80] J. A. Kohlbeck, A study of production grade nitroguanidine for recrystallization to high bulk density nitroguanidine, Proceedings for the Joint International Symposium on Compatibility of Plastics and Other Materials with Explosives, Propellants, Pyrotechnics and Processing of Explosives, Propellants and Ingredients, 23–25 October **1989**, Virginia Beach, VA, USA, pp. 271–277.

[81] L. Desvergnes, Quelques proprietes physiques de certains derives nitres, *Revue de chimie industrielle et le Moniteur scientifique de Quesneville*, **1929**, 265–266.
[82] M. Niehaus, U. Teipel, G. Bunte, H. H. Krause, Suitability of Modified Supercritical Carbon Dioxide as Solvent for Polar Substances, *Propellants Explos. Pyrotech.* **1997**, *22*, 176–179.
[83] D. Powała, A. Orzechowski, A. Maranda, J. Nowaczewski, Spherical Nitroguanidine as Component of High Explosives, *VII. Seminar on New Trends in Research of Energetic Materials*, Pardubice, Czech Republic, 20–22 April **2004**, pp. 606–613.
[84] W. Engel, H. Heinisch, *Verfahren zur Herstellung von kristallinem Nitroguanidin*, DE-Patent 2756335C2, **1982**, Fraunhofer-Gesellschaft e.V., Deutschland.
[85] M. E. Sitzmann, S. C Foti, Solubilities of Explosives – Dimethylformamide as General Solvent for Explosives, *J. Chem. Eng. Data* **1975**, *20*, 53–55.
[86] J. Li, S. Wu, K. Lu, Study on Preparation of Insensitive and Spherical High Bulk Density Nitroguanidine with Controllable Particle Size, *Propellants Explos. Pyrotech.* **2016**, *41*, 312–320.
[87] H. Grau, A. Gandzelko, P. Samuels, Solubility of Raw Materials in Molten 2,4-Dinitroanisole, *Propellants Explos. Pyrotech.* **2014**, *39*, 604–608.
[88] L. Xiao, X. Xing, F. Zhao, H. Gao, L. Na, L. Yang, J. Yi, Thermochemical Properties of Dissolution of Nitroguanidine in Dimethyl Sulphoxide and N.N-Dimethylformamide, *Adv. Mater. Res.* **2013**, *800*, 417–423.
[89] E. J. Pritchard, G. F. Wright, Production of Nitroguanidine with High Bulk Density, *Can. J. Res.* **1947**, *25*, 257–263.
[90] W. Engel, Darstellung von kugeligem Nitroguanidin, *12th International Annual Conference of ICT*, 1–3 July **1981**, Karlsruhe, pp. 21–29.
[91] R. J. Spear, L. D. Redman, R. Barrow, Conversion of Propellant Grade Picrite to spherical Nitroguanidine, *MRL-TR-91-33*, Materials Research Laboratory, Australia, **1991**, 44 pp.
[92] S. Gao, B. Hu, X. Jin, Preparation of Spherical Nitroguanidine by Solvent/non-solvent Method, *Chin. J. Expl. Prop.* **2014**, *37*, 44–47.
[93] J. A. Sanchez, E. L. Roemer, L. A. Stretz, *Spherical Nitroguanidine Process*, US Patent 4967000, **1990**, The United States of America as represented by the Department of Energy, USA.
[94] H. Hommel, Verfahren zum Herstellen von sphärolithischem Nitroguanidin hoher Schütt- und Packungsdichte, insbesondere von kugelig kristallisiertem Nitroguanidin, DE-Patent 3527200C2, **1989**, Fraunhofer-Gesellschaft e.V., Deutschland.
[95] H. Hommel, *Verfahren zur Herstellung von kristallisiertem Nitroguanidin*, DE-Patent 3920999C1, **1990**, Fraunhofer-Gesellschaft e.V., Deutschland.
[96] H. Heinisch, K.-D. Thiel, *Verfahren zur Herstellung von sphärolitischem Nitroguanidin*, DE-Patent 4336049C1, **1995**, Fraunhofer-Gesellschaft e.V., Deutschland.
[97] D. Powała, A. Orzechowski, A. Maranda, J. Nowaczewski, A. Lorek, Researches on New Crystalline Form of Some Insensitive High Explosives in PBX, *Centr. Eur. J. Energ. Mater.* **2004**, *1*, 63–73.
[98] STANAG 4026 JAIS (Ed.3) -*Explosives*, *Specification for Nitroguanidine (Picrite)*, NATO Standardization Agency, Brussels, Belgium, 28 April **2009**.
[99] MIL-N-494A (Notice-2), *Military Specification: Nitroguanidine (Picrite)*, 08 Aug **2013**, Department of the Army, Washington, USA.
[100] Def Stan 07-012 – "*Picrite*", Issue No: 1 dated 11/03/1969, Amendment No: 1 dated 22/11/1974; Information accessed at https://www.dstan.mod.uk on August 13 **2018**.
[101] P. W. Bridgman, Polymorphic transitions up to 50,000 Kg/Cm^2 of several organic substances, *Proc. Am. Acad. Arts Sci.* **1937**, *72*, 227–268.
[102] A. M. Soldate, R. M. Noyes, X-Ray-Diffraction Patterns for the Identification of Crystalline Constituents of Explosives, *Anal. Chem.* **1947**, *19*, 442–444.
[103] W. C. McCrone, Nitroguanidine, *Anal. Chem.* **1951**, *23*, 205–206.
[104] J. E. Abel, P. J. Kemmey, Identification of Explosives by X-Ray Diffraction, *Technical Report 4766*, May **1975**, Picatinny Arsenal, NJ, USA,
[105] E. K. Vasil'ev, A. N. Saposhnikov, Z. A. Dobronravova, L. I. Vereshchagin, Powder Diffraction Data for Nitroguanidine, $(NH_2)_2NNO_2$, *Powder Diffr.* **1991**, *6*, 164–165.
[106] F. H. Allen, O. Kennard, D. G. Watson, L. Brammer, A. G. Orpen, R. Taylor, Tables of Bond Lengths determined by X-Ray and Neutron Diffraction. Part 1. Bond Lengths in Organic Compounds, *J. Chem. Soc. Perkin Trans. II* **1987**, S1–S19
[107] M. Woinska, S. Grabowsky, P. M. Dominiak, K. Woźniak, D. Jayatilaka, Hydrogen atoms can be located accurately and precisely by X-ray crystallography, *Science Advances* **2016**, *2*, e1600192.
[108] H. H. Cady, A. C. Larson, The Crystal Structure of 1,3,5-Triamino-2,4,6-trinitrobenzene, *Acta Cryst.* **1965**, *18*, 485–496.
[109] P. Politzer, J. M. Seminario, P. R. Bolduc, A Proposed Interpretation of the destabilizing effect of hydroxyl groups on nitroaromatic molecules, *Chem. Phys. Lett.* **1989**, *158*, 463–469.
[110] P. Gilinsky-Sharon, H. E. Gottlieb, D. E. Rajsfus, K. Keinan-Adamsky, V. Marks, P. Aped, A. A. Frimer, 1,1-Diamino-2,2-dinitroethylenes are always zwitterions, *Magn. Reson. Chem.* **2012**, *50*, 672–679.
[111] A. D. Vasiliev, A. M. Astachov, M. S. Molokeev, L. A. Kruglyakova, R. S. Stepanov, 1,2-Dinitroguanidine, *Acta Cryst.* **2003**, *C59*, o550–o552.
[112] D. Fischer, T. M. Klapötke, J. Stierstorfer, Energetic materials based on 3,5-diamino-1-nitroguanidine, *15th Seminar on New Trends in Research of Energetic Materials*, 18–20 April **2012**, Pardubice, Czech Republic, pp. 115–127.
[113] S. Nordenson, On Nitroguanidines. II The Structure of N-Methyl-N′-nitroguanidine, *Acta Cryst.* **1981**, *B37*, 1543–1547.
[114] A. M. Astachov, A. A. Nefedov, A. D. Vasiliev, L. A. Kruglyakova, M. S. Molokeev, K. P. Dyugaev, S. V. Trubin, P. P. Semyannikov, R. S. Stepanov, 1,1,3,3-Tetramethyl-2-nitroguandine, *35th International Annual Conference of ICT*, June 29–July 2, **2004**, Karlsruhe, Germany, P-58.
[115] H. N. de Armas, O. M. Peeters, N. Blaton, E. Van Gyseghem, J. Martens, G. Van Haele, G. Van den Mooter, Solid State Characterization and Crystal Structure from X-ray Powder Diffraction of Two Polymorphic Forms of Ranitidine Base, *J. Pharm. Sci.* **2009**, *98*, 146–158.
[116] J. H. Bryden, L. A. Burkhardt, E. W. Hughes, J. Donohue, The crystal structure of Nitroguanidine, *Acta Cryst.* **1956**, *9*, 573–578.
[117] J. P. Ritchie, D. T. Cromer, R. R. Ryan, R. F. Stewart, H. J. Wasserman, Electron density Distribution Analysis for Nitroguanidine, *8th International Detonation Symposium*, 15–19 July **1985**, Albuquerque, NM, USA, pp. 839–846.
[118] A. J. Bracuti, Crystal structure refinement of nitroguanidine, *J. Chem. Cryst.* **1999**, *29*, 671–676.

[119] A. J. Bracuti. Structural features of 2-Nitroguanidine, *Technical Report ARWEC-TR-03004*, Picatinny Arsenal, NJ, USA, June **2003**.

[120] R. K. Murmann, R. Glaser, C. L. Barnes, Structures of nitroso- and nitroguanidine X-ray crystallography and computational analysis, *J. Chem. Cryst.* **2005**, *35*, 317–325.

[121] R. A. Wiscons, A. J. Matzger, Evaluation of the Appropriate Use of Characterization Methods for Differentiation between Co-crystals and Physical Mixtures in the Context of Energetic Materials, *Cryst. Growth Des.* **2017**, *17*, 901–906.

[122] X. Wie, A. Zhang, Y. Ma, X. Xue, J. Zhou, Y. Zhu, C. Zhang, Toward low-sensitive and high-energetic co-crystal III: thermodynamics of energetic-energetic co-crystal formation, *CrystEngComm* **2015**, *17*, 9037–9047.

[123] H. J. Lloyd, C. R. Pulham, R. Doherty, A review of co-crystals, *18th Seminar on New Trends in Research of Energetic Materials*, Pardubice, Czech Republic, 15–17 April **2015**, pp. 178–187.

[124] K. S. Hope, H. J. Lloyd, D. Ward, A. A. L. Michalchuk, C. R. Pulham, Resonant acoustic mixing: Its applications to energetic materials, *18th Seminar on New Trends in Research of Energetic Materials*, Pardubice, Czech Republic, 15–17 April **2015**, pp. 134–143.

[125] K. S. Hope, D. Ward, H. J. Lloyd, S. Hunter, C. L. Bull, C. R. Pulham, Putting the squeeze on energetic co-crystals: High-Pressure studies of 2 (CL-20) : HMX and NQ : DNP, *19th Seminar on New Trends in Research of Energetic Materials*, Pardubice, Czech Republic, 20–22 April **2016**, pp. 132–140.

[126] K. Hope, University of Edinburgh, UK, *personal communication*, August **2018**.

[127] H. Gao, P. Du, X. Ke, J. Liu, G. Hao, T. Chen, W. Jiang, A Novel Method to Prepare Nano-sized CL-20/NQ co-crystal: Vacuum Freeze Drying, *Propellants Explos. Pyrotech.* **2017**, *42*, 889–895.

[128] H. Gao, Q. Wang, X. Ke, J. Liu, G. Hao, L. Xiao, T. Chen, W. Jiang, Q. Liu, Preparation and characterization of an ultrafine HMX/NQ co-crystal by vacuum freeze drying method, *RSC Adv.* **2017**, *7*, 46229–46235.

[129] K. Liu, G. Zhang, C. Gao, W. Zhiqun; M. Wang, J. Luan, Q. Pan, X. Qing, L. Min, Z. Xiaoyu; L. Zhang, *Co-crystal explosive of hexanitrohexaazaisowurtzitane and nitroguanidine, and its preparation method*, CN-Patent 108101722, **2018**, China.

[130] T. H. Lee, R. J. Colton, M. G. White, J. W. Rabalais, Electronic Structure of Hydrazoic Acid and the Azide Ion from X-Ray and Ultraviolet Electron Spectroscopy, *J. Am. Chem. Soc.* **1975**, *97*, 4845–4851.

[131] T. H. Lee, J. W. Rabalais, X-Ray photoelectron spectra and electronic structure of some diamine compounds, *J. Electron. Spectrosc. Relat. Phenom.* **1977**, *11*, 123–127.

[132] B. C. Beard, Cellulose nitrate as a binding energy reference in N(1 s) XPS studies of nitrogen-containing organic molecules, *Appl. Surf. Sci.* **1990**, *45*, 221–227.

[133] J. Sharma, W. L. Garrett, F. J. Owens, V. L. Vogel, X-ray Photoelectron Study of Electronic Structure and Ultraviolet and Isothermal Decomposition of 1,3,5-Triamino-2,4,6-trinitrobenzene, *J. Phys. Chem.* **1982**, *86*, 1657–1661.

[134] M. Piskorz, T. Urbański, Ultraviolet and Infrared Spectra of Some Nitramines, *Bull. Acad. Pol. Sci.* **1963**, *XI*, 615–624.

[135] F. H. Bissett, L. A. Levasseur, Analytical methods for Nitroguanidine and Characterization of its Degradation products, *TR 76–47*, Food Science Laboratory, Natick MS, USA, **1976**, 17 pp.

[136] N. S. Morozova, E. L. Metelkina, T. A. Novikova, V. A. Shlyapochnikov, O. I. Sergienko, V. V. Perekalin, Interpretation of vibrational spectra of nitroguanidine, *Zhu. Org. Chim.* **1983**, *19*, 1228–1232.

[137] K. L. McNesby, J. E. Wolfe, J. B. Morris, R. A. Pesce-Rodriguez, Fourier Transform Raman Spectroscopy of Some Energetic Materials and Propellant Formulations, *J. Raman Spectrosc.* **1994**, *25*, 75–87.

[138] J. Hwang, N. Choi, A. Park, J.-Q. Park, J. H. Chung, S. Baek, S. G. Cho, S.-J. Baek, J. Choo, Fast and sensitive recognition of various explosive compounds using Raman spectroscopy and principal component analysis, *J. Mol. Struct.* **2013**, *1039*, 130–136.

[139] J. Chen, Y. Chen, H. Zhao, G. J. Bastiaans, X.-C. Zhang, Absorption coefficients of selected explosives and related compounds in the range of 0.1–2.8 THz, *Opt. Express* **2007**, *15*, #83695.

[140] N. Palka, M. Szala, Transmission and Reflection Terahertz Spectroscopy of Insensitive Melt-Cast High-Explosive Materials, *J. Infrared Milli. Terahz. Waves* **2016**, *37*, 977–992.

[141] T. R. Juliano, Jr., M. D. King, T. M. Korter, Evaluating London Dispersion Force Corrections in Crystalline Nitroguanidine by Terahertz Spectroscopy, *IEEE Trans. Terahertz Sci. Technol.* **2013**, *3*, 281–287.

[142] R. E. Richards, R. W: Yorke, A Proton Magnetic Resonance Investigation of the Structure of Nitroguanidine, *Trans. Faraday Soc.* **1958**, *54*, 321–326 .

[143] A. H. Lamberton, I. O. Sutherland, J. E. Thorpe, H. M. Yusuf, Nitramines and Nitramides. Part XIII. Nuclear Magnetic Resonance Spectra, *J. Chem. Soc.* **1968** (*B*), 6–8.

[144] A. M. Astachov, P. V. Brovchenko, W. A. Skolenko, G. E. Salnikov, A. I. Rubailo, New NMR data of molecular dynamic of nitroguanidine, *14th Seminar on New Trends in Research of Energetic Materials*, Pardubice, Czech Republic, 13–15 April **2011**, pp. 458–463.

[145] L. Šimkova, M. Šoral, K. Lušpai, J. Ludvík, Spectroscopic characterization of different structural forms of the new promising energetic material FOX-7 in different solvents, *J. Mol. Struct.* **2015**, *1083*, 10–16.

[146] J. Gálvez, A. Guirado, A Theoretical Study of Topomerization of Imine Systems: Inversion, Rotation or Mixed Mechanisms? *J. Comput. Chem.* **2010**, *31*, 520–531.

[147] H. Kessler, D. Leibfritz, Nachweis Innermolekularer Beweglichkeit durch NMR-Spektroskopie – XV Untersuchungen zur Inversion am Doppelt Gebundenen Stickstoffatom am Beispiel der Tetramethylguanidine, *Tetrahedron* **1970**, *26*, 1805–1820.

[148] H. Kessler, D. Leibfritz, Nachweis Innermolekularer Beweglichkeit durch NMR-Spektroskopie – XVIII Vergleich der Inversionsgeschwindigkeiten am doppelt gebundenen Stickstoff bei Guanidinen und Imidazolidiniminen, *Liebigs Ann. Chem.* **1970**, *737*, 53–60.

[149] H. Günther, *NMR-Spektroskopie*, Thieme-Verlag, Stuttgart, 2. Ed. **1983**, p. 14.

[150] S. Bulusu, R. L. Dudley, J. R. Autera, Structure of Nitroguanidine: Nitroamine or Nitroimine? New NMR Evidence from ^{15}N-Labeled Sample and ^{15}N Spin Coupling Constants, *Magn. Reson. Chem.* **1987**, *25*, 234–238.

[151] G. R. Bedford, P. J. Taylor, G. A. Webb, ^{15}N-NMR-Studies of Guanidines, *Magn. Reson. Chem.* **1995**, *33*, 383–388.

[152] I. D. Cunningham, N. C. Wan, ^{13}C and ^{15}N NMR Study of Electron Distribution in *N*-Aryl-*N'*-cyanoguanidines, *Magn. Reson. Chem.* **1996**, *34*, 221–226.

[153] H.-O. Kalinowski, S. Berger, S. Braun, *^{13}C-NMR-Spektroskopie*, Thieme Verlag, Stuttgart, **1984**, p. 513–518.

[154] J. B. Miller, Quadrupole Resonance Detection of Explosives in J. Yinon (Ed.) *Counterterrorist Detection Techniques of Explosives*, Elsevier, Amsterdam, **2007**, 157–198.

[155] C. Spyckerelle, G. Eck, P. Sjöberg, A.-M. Amnéus, Reduced Sensitivity RDX Obtained From Bachmann RDX, *Propellants Explos. Pyrotech.* **2008**, *33*, 14–19.
[156] D. McAteer, J. Akhavan, Nitrogen-14 NMR Spectroscopic Detection of Explosophores in Solution, *Propellants Explos. Pyrotech.* **2016**, *41*, 367–370.
[157] J. H. Beynon, J. A. Hopkinson, A. E. Williams, The Mass Spectra of some Guanidines, *Org. Mass Spectrom.* **1968**, *1*, 169–187.
[158] F. Volk, H. Schubert, Massenspektrometrische Untersuchungen von Explosivstoffen, *Explosivstoffe* **1968**, *16*, 2–10.
[159] A. P. Glazkova, Effect of Catalysts on the Combustion of Nitroguanidine and Ammonium nitrate -Nitroguanidine Mixtures, *Comb. Explos. Shock Waves* **1973**, *7*, 177–185.
[160] E.-C. Koch, Extrem Insensitive Detonierende Stoffe, EIDS, Testverfahren und Materialien, *Seminar – Insensitive Munition*, Bundesakademie für Wehrverwaltung und Wehrtechnik, Mannheim, 30 June–2 July, **2008**.
[161] United Nations, *Transport of Nitroguanidine, wetted, (UN 1336) in flexible IBCs*, ST/SG/AC.10/C.3/2006/52, Geneva, 13 April **2006**. Accessed on August 13 2018 at https://www.unece.org/fileadmin/DAM/trans/doc/2006/ac10c3/ST-SG-AC10-C3-2006-52e.pdf.
[162] United Nations, Recommendations on the Transport of Dangerous Goods, Manual of Tests and Criteria, 6th revised edition, Geneva, Switzerland, **2015**.
[163] T. R. Gibbs, A. Popolato, *LASL Explosive Property Data*, University of California Press, Berkeley, **1980**, p. 60.
[164] H. Henkin, R. McGill, Rates of Explosive Decomposition of Explosives, *Ind. Eng. Chem.* **1952**, *44*, 1391–1395.
[165] L. C. Myers, Henkin Time-to-Explosion for TATB – Part I, *MHSMP-77-18H*, Mason and Hanger-Silas Mason Co., Inc., Amarillo, TX (USA), **1977**.
[166] J. Maienschein, Cookoff Violence Prediction at LLNL: Experimental Approaches Past, Present, and Future, Lawrence Livermore National Laboratory, CA, USA, *Cookoff Workshop*, NAWC China Lake,Ridgecrest, CA, USA, March 12–13, **1996**.
[167] B. Janzon, H. Bergman, C. Eldsäter, C. Lamnevik H. Östmark, FOX-7 – A Novel, High Performance, Low Vulnerability High Explosive for Warhead Applications, *20th Ballistic Symposium*, 23–27 September **2002**, Orlando, FL, USA,.
[168] H. Koenen, K. H. Ide, Über die Prüfung explosive Stoffe (II), *Explosivstoffe* **1956**, *4*, 143–148.
[169] H. Flower, C. Stennett, S. Wortley, Hazard Characterization of FOX-7 Compositions with Varying Particle Sizes, *14th Detonation Symposium*, Coeur d'Alene, ID, USA, 11–16. April **2010**, pp. 1372–1378.
[170] D. Price, Gap Tests and How they Grow, *22nd Explosives Safety Seminar*, Anaheim, CA, USA, 26–28 August **1986**, pp. 365–380.

Manuscript received: August 17, 2018
Revised manuscript received: October 21, 2018
Version of record online: January 18, 2019

